STUDY OF VIBRATIONAL ENERGY EXCHANGE AND DETERMINATION OF V-V EXCHANGE RATE CONSTANTS ON HIGH LEVELS OF THE CO MOLECULE

Final Report on Contract F61775-98-WE058

Sponsored by the

US Air Force Research Laboratory, Kirtland AFB, NM, and the

European Office of Aerospace Research and Development, London, England

SPC-98-4038

April 1998-April 1999

P.N.Lebedev Physics Institute, Moscow, Russia

Principal investigator, Scientific leader
Prof.A.Ionin

Investigators:
Mr.D.Sinitsyn
Mr.YuKlimachev
Mr.L.Seleznev
Mr.A.Kotkov

Troitsk Institute for Innovation and Fusion Research, Troitsk, Moscow Region, Russia

Scientific leader
Prof.A.Napartovich

Investigator:
Dr.A.Kurnosov

Institute of High Temperatures, Moscow, Russia

Scientific leader
Prof.Yu.Konev

Moscow
1999

REPORT DOCUMENTATION PAGE

Form Approved OMB No. 0704-0188

1. AGENCY USE ONLY (Leave blank)	2. REPORT DATE	3. REPORT TYPE AND DATES COVERED
	1999	Final Report

4. TITLE AND SUBTITLE

Study of Vibrational Energy Exchange and Determination of V-V Exchange Rate Constants on High Levels of the CO Molecule

5. FUNDING NUMBERS

F61775-98-

6. AUTHOR(S)

Dr. Andre Ionin

7. PERFORMING ORGANIZATION NAME(S) AND ADDRESS(ES)

P. N. Lebedev Physical Institute
53 Leninsky Prospect
Moscow 117924
Russia

8. PERFORMING ORGANIZATION REPORT NUMBER

N/A

9. SPONSORING/MONITORING AGENCY NAME(S) AND ADDRESS(ES)

EOARD
PSC 802 BOX 14
FPO 09499-0200

10. SPONSORING/MONITORING AGENCY REPORT NUMBER

SPC 98-4038

11. SUPPLEMENTARY NOTES

12a. DISTRIBUTION/AVAILABILITY STATEMENT

Approved for public release; distribution is unlimited.

12b. DISTRIBUTION CODE

A

13. ABSTRACT (Maximum 200 words)

This report results from a contract tasking P. N. Lebedev Physical Institute as follows: The contractor will obtain new information concerning the kinetics of energy exchange between highly excited CO molecules A new theoretical model of CO vibrational kinetics will be verified on the basis of laser energy output measurements from a frequency-selective, double-pulsed, Q-switched CO laser. These energy mesurements will be used to infer rate constants, and these constants will be used to predict the operation of CO lasers that are based on using highly excited CO molecules.

14. SUBJECT TERMS

EOARD, CO lasers, Aerophysics of Ionized Gases, Computational Fluid Dynamics, gas lasers, High average power gas lasers, High Temperature Kinetics

15. NUMBER OF PAGES

44

16. PRICE CODE

N/A

17. SECURITY CLASSIFICATION OF REPORT	18. SECURITY CLASSIFICATION OF THIS PAGE	19. SECURITY CLASSIFICATION OF ABSTRACT	20. LIMITATION OF ABSTRACT
UNCLASSIFIED	UNCLASSIFIED	UNCLASSIFIED	UL

1. INTRODUCTION

In many areas of research activity such as high speed non-equilibrium gas dynamics, plasma chemistry, isotope separation, atmosphere physics, laser physics, etc., a detailed knowledge of vibrational energy exchange kinetics of highly excited molecules is required. It is a central point of computer modeling of CO lasers. It is important for practical use of laser devices, such as overtone CO laser, frequency selective CO laser, optically pumped CO laser, Q-switched CO laser, operation of which is based on processes involving highly excited CO molecules. A prediction of their operation is very sensitive to details of vibrational kinetics.

Computer modeling of vibrational kinetics is a powerful tool of system analysis. There are two alternative models of CO molecule vibrational kinetics.

The first and widely used one is based on simplified single quantum VV exchange (SQE) model [1-4]. A set of rate constants for single quantum processes $CO(\mathbf{v})+CO(\mathbf{u})\rightarrow CO(\mathbf{v}\text{-}1)+CO(\mathbf{u}+1)$, included in calculations, is verified experimentally only for low vibrational levels **v** and **u**. Rate constants for high vibrational levels are found by extrapolation procedure. The first order perturbation theory expressions are used for the extrapolation [1-4]. This procedure was never verified for calculations of VV-exchange rates of highly excited CO molecules. In particular, rate coefficients grow rapidly with an increase of **v** and **u** and exceed the gas kinetic value at rather low $\mathbf{v},\mathbf{u}>6\text{-}7$ for quasi-resonance exchange. Nevertheless, rate constants, obtained by this way, have been commonly used in practical calculations. Their justification is based on rather satisfactory agreement with measurements of stationary vibrational distribution function (VDF) available in literature.

The second model takes into consideration multi-quantum vibration exchange (MQE). As it follows from basic quantum mechanical principles [5, 6], multi-quantum exchange processes

$$CO(\mathbf{v})+CO(\mathbf{u})\text{-->}CO(\mathbf{v}\text{-}\mathbf{n})+CO(\mathbf{u}+\mathbf{n}) \qquad (1)$$

become significant, when probabilities of (**n**-1)-quantum processes reach a value of an order of unity (**n** is the number of quanta exchanged). As was shown in [6], the rate constants of processes (1) ($\mathbf{n}\geq 2$) become of nearly the same value as single-quantum rate constants in the range of vibrational quantum numbers exceeding $\mathbf{v}=10$. A set of the rate constants from [6], given at low temperature T=100 K for vibrational levels $\mathbf{v}>5$, was incorporated in CO vibrational kinetics model and resulted in satisfactory agreement with experimental data on measurement of stationary VDF [7, 8]. The calculations [7, 8] also demonstrated that transient behavior of the VDF after frequency selective perturbation is quite different in both models for high vibrational levels, but very similar for lower levels. An experimental verification of the model in respect to non-stationary VDF or laser devices has not been performed till now.

The main objective of the project is to verify the model of CO laser active medium taking into account MQE processes. A mean of the verification is a set of experimental data on measurements of laser pulse energy restoration time for double pulse Q-switching mode of frequency selective CO laser

[9,10] operating on high vibrational levels. The only source of our knowledge on MQE rate constants is numerical calculations performed by Billing with co-authors, based on semi-classical considerations, which were reviewed in details in [6]. It was supposed, on the base of our experimental data, to get new information in support of the rate constants [6] and to make an attempt to get more precise knowledge of MQE rate constants. On the base of these results, having fundamental physical value, it was supposed also to use the MQE model in studies of a first overtone (FO) CO laser operating both in free running mode and in frequency selective mode. It is very important, because CO overtone lasing takes place on high vibrational levels where an applicability of the SQE model of VV exchange is in doubt.

The Report is arranged as follows. Section 2 presents a state of the problem. A description of the MQE CO laser kinetic model is given in Section 3. A description of methodological tools of the experiments and their results are presented in Section 4. An analysis of experimental results and a comparison with results of modeling including calculations of FO CO laser characteristics are performed in Section 5. A summary of the research and suggestions for further research work are presented in Section 6.

2. THE STATE OF THE PROBLEM

The SQE model of CO laser is summarized in details in [11]. It includes, besides SQE VV exchange rate constants, detailed information on all important processes, that is, electron-molecule excitation rates, rates of VT relaxation, spontaneous and induced radiative processes, spectroscopic data and the equation for gas temperature.

Rate constants for VV exchange in the SQE model are usually calculated using expressions, based on the first order perturbation theory assumptions. The expressions are derived in the approximation [1], where long- and short-range forces act independently, and the results are summed. The parameters of the theoretical expressions are usually fitted to get the dependencies on magnitude and vibrational quantum number of those rate constants, which were measured experimentally. The rate constants, extrapolated by this way to VV-exchange of highly excited molecules, grow rapidly with an increase of **v** and **u** and exceed the gas kinetic value at rather low **v,u**>7 for quasi- resonance exchange. Strictly speaking, a validity of the first order perturbation theory expressions is broken down and vibration kinetic models using these rate constants are questionable for relatively low levels. Nevertheless, the rate constants, obtained by the way mentioned above, have been widely used in practical calculations. Their validity was explained by a satisfactory agreement with measurements of VDF available in literature (for example, see an excellent paper [12]).

The validity of SQE rate constants [1-4, 11] has been discussed in the literature since the paper [3] was published, where rate constants of exothermic processes were proposed to be limited by the gas kinetic value. However, a realization of this simplified procedure showed a poor agreement with measured stationary VDF values.

The theoretical papers [5, 6] made more realistic assumptions on VV exchange in CO. The quasi-resonant single quantum VV exchange rate constants, as calculated by Billing [6], do not exceed gas kinetic value. The Billing's rate constants, when incorporated in the SQE kinetic model, also bring forth the VDF values strongly differing from those obtained by measurements.

An analytic approach to the theory of vibrational quanta exchange was developed in papers [13, 14] and in publications cited there as well. This theory might be useful to obtain scaling laws for rate constants dependence on vibration quantum numbers and temperature and to get more deep insight into the processes. In particular, exponential dependencies of cross sections on the energy of colliding molecules and temperature were derived. But practically, to get parameters of analytic approximations of cross sections, it is necessary to do detailed trajectory calculations, similar to those presented in [6]. This work has never been done.

Thus, the only information source on MQE rate constants available to us is publication [6] with summarized Billing's data. The data in Ref. [6] are presented for a number of selected processes at **T**=100 K, 200 K, 300 K, 500 K and 1000 K. Only a few data points are given for three- and four-quantum exchange. Table 1 represents Billing's data on **m**-quantum exchange rate constants in CO for

selected gas temperatures. One should admit heuristic considerations, which are not well grounded, to estimate all elements of a matrix composed of rate constants in kinetic equations. Some considerations on this matter are presented in [15] for single-quantum exchange. An approach in [15] is an essentially formal statistical one. It may be used for single-quantum exchange constant estimations. But because of the lack of data and absence of a physical background it may be recommended for multi-quantum exchange description.

In the next Section MQE CO laser kinetic model is presented as developed by authors of this research.

Table 1. Rate constants of **m**-quantum exchange in CO [6]

u v→u' v'	ΔE, cm^{-1}	100 K	200 K	300 K	500 K
6 6→4 8	102.9	1.64E-11	0.68E-11	4.1E-12	2.2E-12
8 6→6 10	101.4	2.85E-11	1.49E-11	1.00E-11	6.0E-12
10 10→8 12	100.0	4.64E-11	2.62E-11	1.82E-11	1.14E-11
10 10→7 13	224.8	4.7E-12	1.9E-12	1.6E-12	1.0E-12
10 8→12 6	201.3	4.11E-12	4.15E-12	5.25E-12	5.88E-12
10 12→12 10	0.0	1.07E-11	7.3E-12	7.3E-12	7.9E-12
10 6→12 4	304.2	1.05E-13	1.71E-13	3.54E-13	8.04E-13
12 12→10 14	98.5	5.54E-11	3.72E-11	2.98E-11	2.32E-11
13 13→11 15	97.8	6.31E-11	4.36E-11	3.59E-11	2.90E-11
14 14→12 16	97.0	6.68E-11	4.51E-11	3.65E-11	2.73E-11
15 15→13 17	96.2	7.40E-11	5.35E-11	4.69E-11	4.13E-11
15 13→13 15	0.0	2.07E-11	1.50E-11	1.54E-11	1.73E-11
15 17→13 19	120.9	2.55E-11	2.86E-11	3.39E-11	3.69E-11
15 19→13 21	284.2	3.56E-12	6.87E-12	1.30E-11	2.40E-11
18 18→16 20	94.0	7.35E-11	6.03E-11	5.95E-11	5.99E-11
18 20→20 18	0.0	3.72E-11	2.94E-11	3.06E-11	3.62E-11
20 20→18 22	92.5	7.39E-11	7.29E-11	7.38E-11	6.73E-11
20 20→17 23	208.2	5.14E-11	3.29E-11	2.57E-11	1.97E-11
20 22→18 24	182.6	7.75E-11	6.25E-11	6.62E-11	6.91E-11
20 24→18 26	273.1	1.49E-11	2.08E-11	3.48E-11	5.56E-11
22 22→20 24	91.0	7.55E-11	7.85E-11	8.19E-11	7.71E-11
24 24→22 26	89.6	7.24E-11	8.01E-11	8.46E-11	8.16E-11
26 26→24 28	88.2	6.92E-11	7.63E-11	7.99E-11	7.86E-11
28 28→26 30	86.6	6.58E-11	6.90E-11	7.06E-11	7.11E-11
30 30→28 32	85.0	5.99E-11	6.22E-11	6.34E-11	6.61E-11
30 30→27 33	191.6	8.89E-11	5.99E-11	5.61E-11	5.58E-11
30 30→26 34	340.5	5.45E-11	3.93E-11	3.52E-11	2.96E-11

3. KINETIC MODEL

3.1. General description of kinetic model.

Except VV exchange processes in CO, a kinetic model is described in [3, 16] and presented in [11]. Thus, only that part of the kinetic model, which represents VV exchange, is described in this Section below. Schematically, the system of kinetic equations, describing a time evolution of CO molecule population on vibrational level **v**, has the form:

$$\frac{dn_v}{dt} = R^v_{e-V} + R^v_{VV} + R^v_{VV'} + R^v_{VT} + R^v_{SP} + R^v_{IND} \qquad (2)$$

Here R^v_{e-V}, $R^v_{VV'}$, R^v_{VT}, R^v_{SP}, R^v_{IND} are the rates of electron-molecule excitation, inter-molecular vibration-vibration exchange, vibration relaxation, spontaneous and induced radiative transitions. Their detailed expressions can be found in [3, 16] and are not presented here. The rates of multi-quantum VV exchange are:

$$R^v_{VV} = \sum_{m\geq 1}(W_{v+m,v}n_{v+m} + W_{v-m,v}n_{v-m} - (W_{v,v+m} + W_{v,v-m})n_v \qquad (3)$$

where $W_{v+m,v}$ is the frequency of transitions from level **v+m** to level **v** in processes of type (1), expressed as follows:

$$W_{v+m,v} = \sum_{i\geq m} Q^{v+m,v}_{i-m,i} n_i \qquad (4)$$

where $Q^{v+m,v}_{i-m,i}$ are the rate constants of **m**-quantum exchange. As one may conclude from [6], processes with **m**>4 are not important for **v**< 30-35 and are not considered.

3.2. Single-quantum exchange constants

For lower vibrational levels, effects of anharmonicity and, hence, effects of multi-quantum exchange play a negligible role. Therefore, for **v**-numbers **v**<5 rate constants were taken in accordance with recommendations of [11], i.e. within the framework of the SQE model. For **v**≥5 all processes were divided into near-resonant and non-resonant ones in the following manner. Collisions between molecules occupying levels with numbers **v** and **v'** were specified as the near-resonant for |**v-v'**|≤5 otherwise they were considered as non-resonant ones. For near-resonant exothermic processes

$$CO(v\text{-}m) + CO(v\text{-}1) \rightarrow CO(v\text{-}m\text{-}1) + CO(v) \qquad (5)$$

rate constants were presented in the form:

$$Q^{v-1,v}_{v-m,v-m-1} = Q^{v-1,v}_{v-1,v-2}\Phi(v,m) \qquad (6)$$

Billing's data allowed us to determine function $\Phi(v,m)$ only for a few selected **v** numbers. At T=100 K this function is given in the Table 2.

Table 2.

m	1	2	3	4	5	6
$\Phi(v=6,m)$	1	0.6406	0.2656	0.0719	0.0156	-
$\Phi(v=11,m)$	1	0.8333	0.5333	0.2750	0.1167	0.045
$\Phi(v=16,m)$	1	0.9375	0.8125	0.5563	0.3125	0.125

At intermediate **v** numbers Φ function was interpolated linearly. For **v**>16 it was proposed to be constant. A similar procedure was realized for a calculation of Φ at gas temperature **T**=200K and 300K. Rate constants calculated in this manner we also call as Billing's rate constants. These rate constants were used in the model for **v**≥10. Finally, in the range 10≥**v**≥5 rate constants were calculated as a linear superposition of Billing's rate constants and those from [11] with numerical coefficients varying from 0 to 1 and opposite, respectively. Such a procedure allowed us to smooth a transition from Billing's rate constants to traditional rate constants collected in [11].

The rate constants for non-resonant processes are much smaller in magnitude and were calculated using formulas presented in [11]. Their magnitudes were normalized using continuity condition to overlap with Billing's rate constants and a linear logarithmic interpolation:

$$\ln Q^{v,v+1}_{w,w-1} = \ln Q^{v,v+1}_{1,0} + (\ln Q^{v,v+1}_{v-5,v-6} - \ln Q^{v,v+1}_{1,0})(w-1)/(v-6) \qquad (7)$$

where $Q^{v,v+1}_{v-5,v-6}$ are Billing's rate constants and $Q^{v,v+1}_{1,0}$ are rate constants from [11], 1≤**w**≤**v**-5.

Fig. 1 and Fig. 2 show SQE rate constants $Q^{v-1,v}_{u,u-1}$ at **T**=100 K and **T**=300 K.

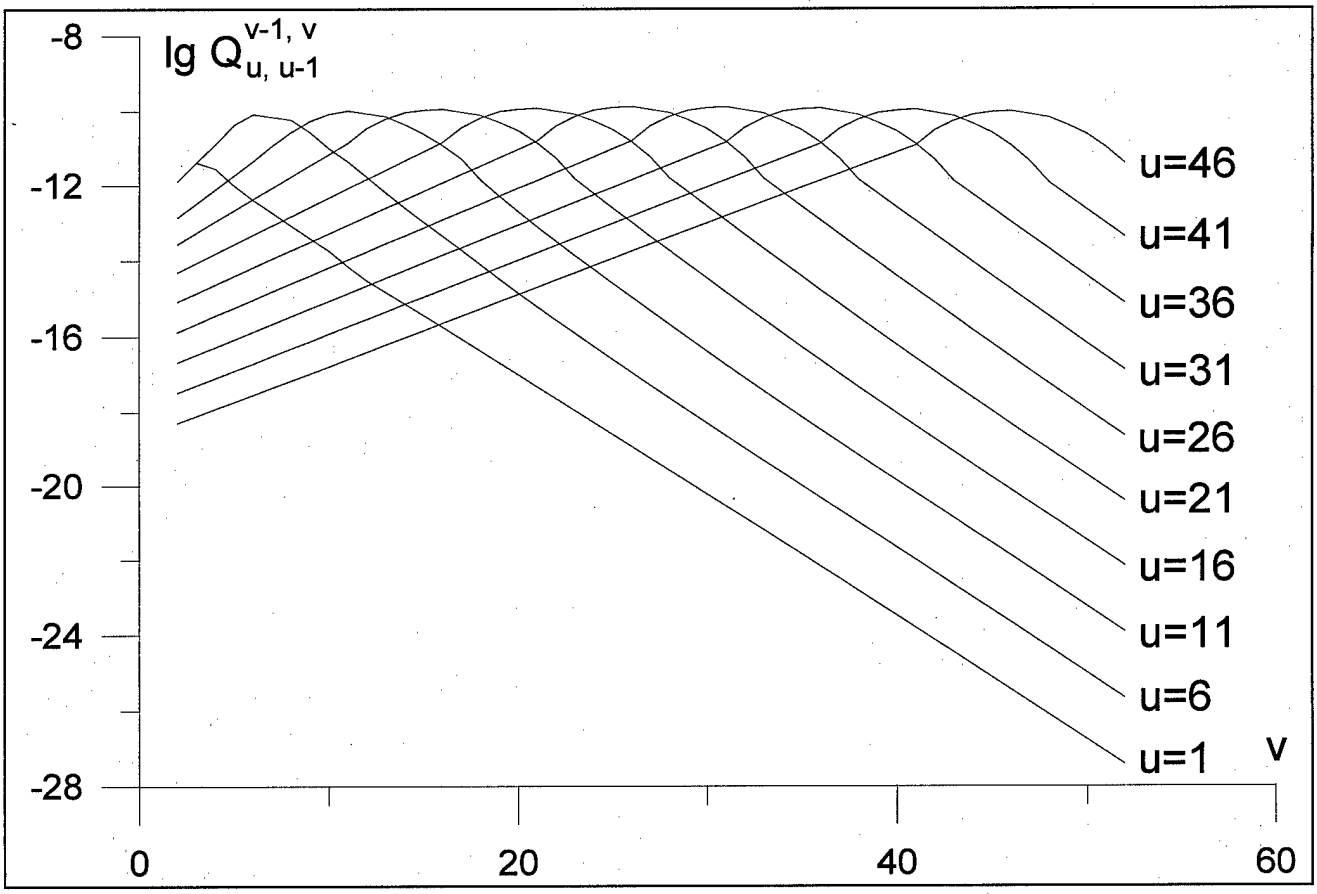

Fig. 1. SQE rate constants at T=100 K, [11]

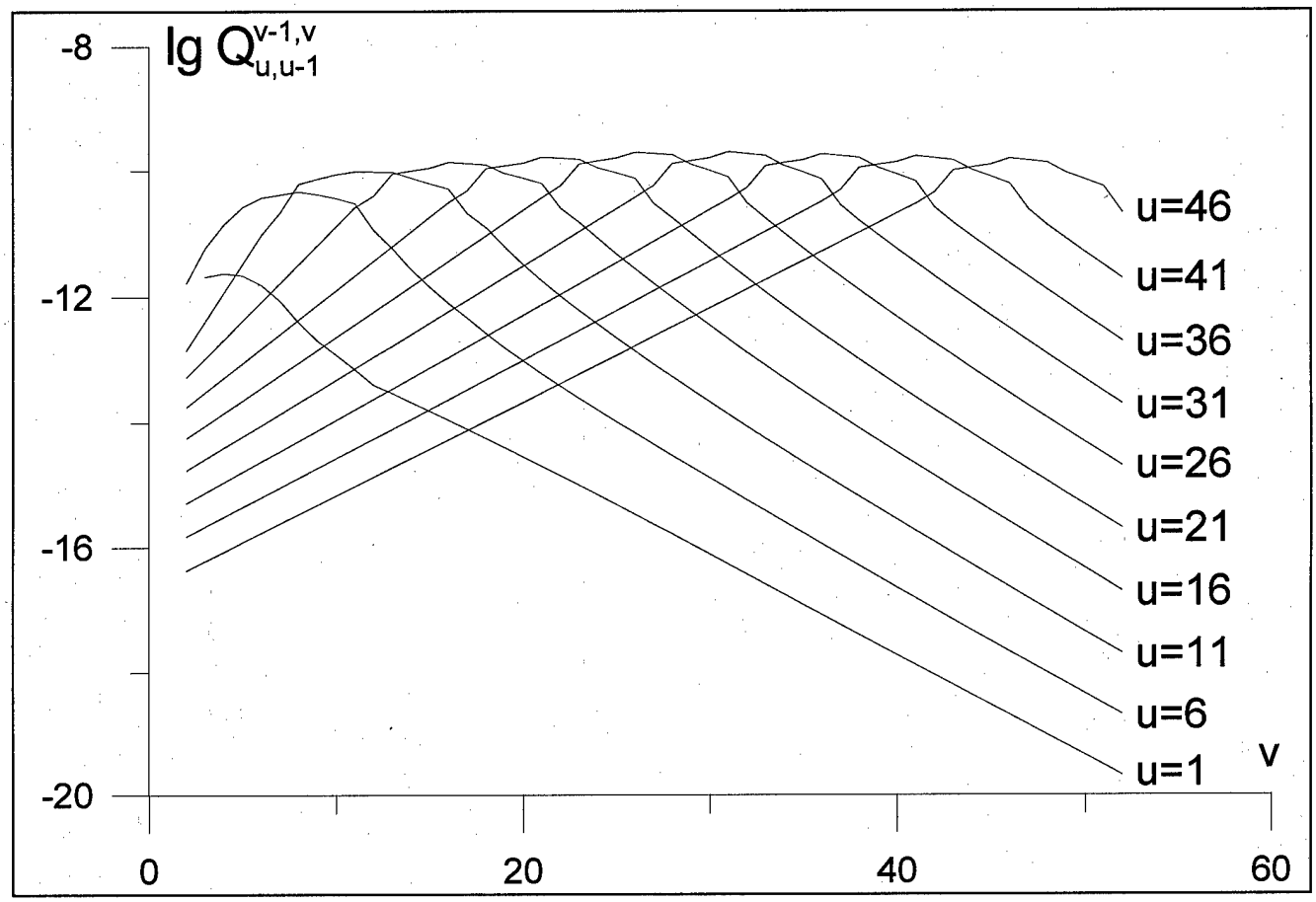

Fig. 2. SQE rate constants at T=300 K, [11]

3.3. Multi-quantum exchange

Analysis of Billing's data allows us to select, for each number of quanta exchanged, the range of **v**-numbers, where multi-quantum transition probabilities are high, that is of an order of unity. Such processes are considered as near-resonant ones. Out of this range processes are defined as non-resonant. Non-resonant range **v**-numbers were considered to be for all $v - u \geq 6$.

Transition probabilities are small for non-resonant processes and supposed to follow SSH perturbation theory [17]. The perturbation theory gives the following dependence of rate constants on initial and final quantum numbers **v** and **u** and the number of exchanged quanta **m**:

$$Q^{u,u+m}_{v,v-m} \sim \left|\frac{q_{v,v-m}}{q_{m,0}}\right|^2 \left|\frac{q_{u,u+m}}{q_{m,0}}\right|^2 F(\Delta E^{v,v-m}_{u,u+m}), \qquad (8)$$

where F(ΔE) is an adiabaticity function for non-resonant processes, which has a universal form in the SSH theory (see, for example [3, 11]), $\Delta E^{v,v-m}_{u,u+m}$ is energy defect of process, $q_{v,v-m}$ is the matrix element of the lowest order interaction term giving rise to a process of **m** quantum exchange. These matrix elements can be calculated using relative value of appropriate Einstein coefficients A and frequency of transitions ν:

$$A_{v,v-m} \sim \left| \frac{q_{v,v-m}}{q_{m,0}} \right|^2 \nu^3_{v,v-m} \qquad (9)$$

Einstein coefficients A for transitions in CO molecule are presented, for example, in [3, 11].

For resonant two-quantum exothermic processes Billing's data allowed us to determine Φ function just in the same manner as for single-quantum processes. For resonant three- and four-quantum processes Billing's data are scarce, and the rate constants for exothermic processes were considered to be constant and equal to the corresponding Billing's rate constants. Non-resonant rate constants were normalized by equalizing to the boundary Billing's rate constants in resonance range. In addition, the rate constants were considered to be zero in the range $v \leq 9$ for two-quantum processes, $v \leq 10$ - for three-quantum processes and $v \leq 15$ for four-quantum processes.

The rate constants were determined for temperatures **T**=100 K, 200 K, 300 K. At intermediate temperatures the rate constants were calculated by means of linear logarithmic interpolation. The rate constants for endothermic processes were found using detailed balance principle.

The rate constants for two-, three- and four-quantum processes at **T**=100K are shown in Figs.3-5.

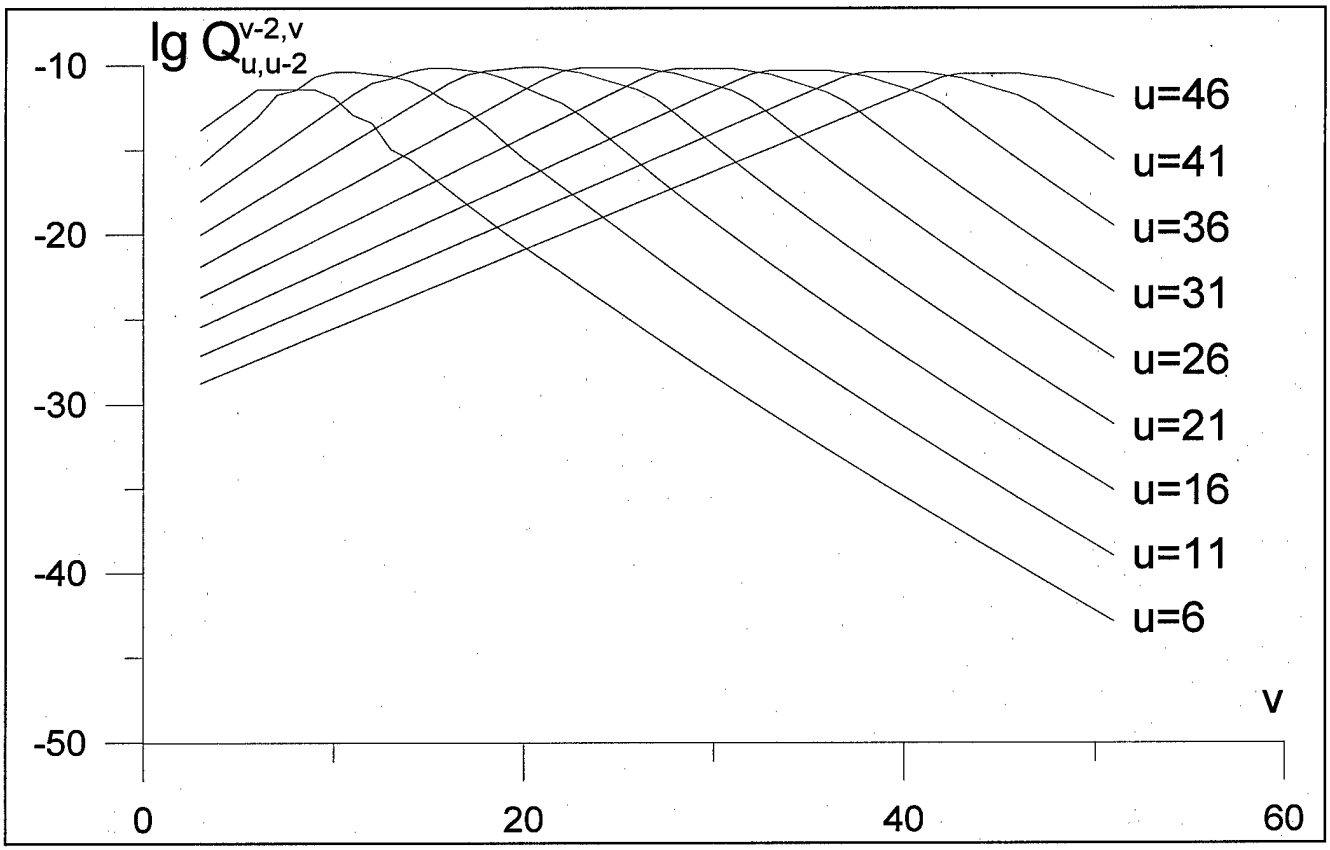

Fig. 3. Two-quantum exchange rate constants, T=100 K

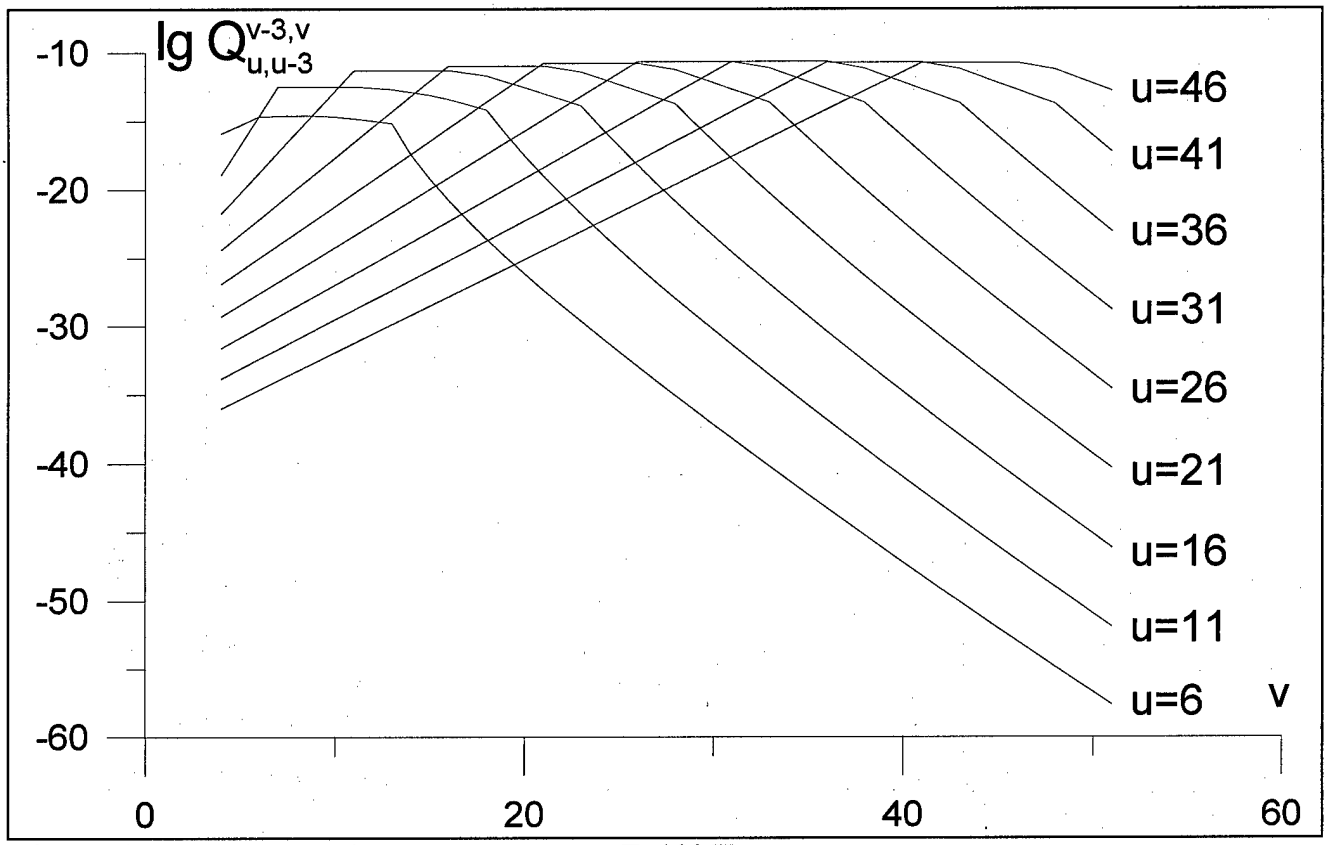

Fig. 4. Three-quantum exchange rate constants, T=100 K

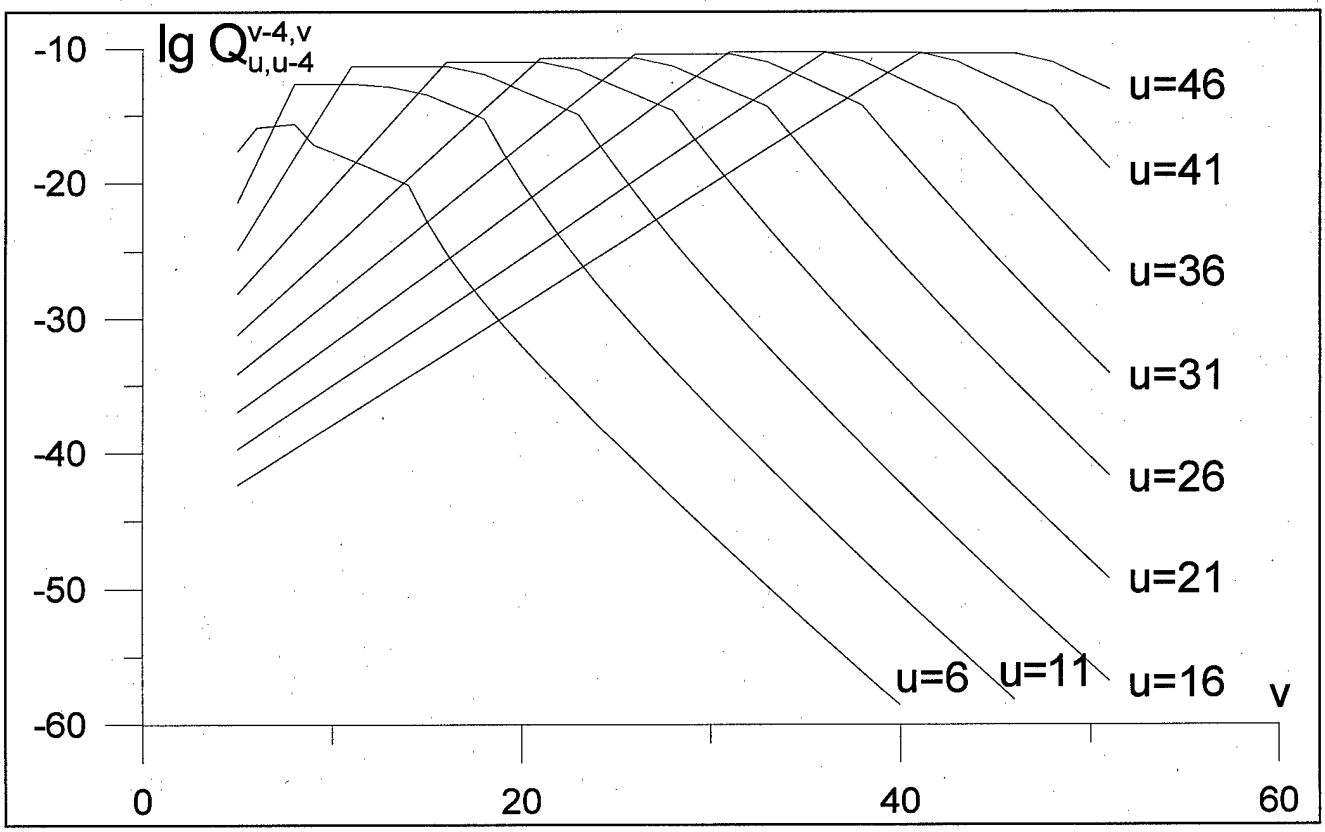

Fig. 5. Four-quantum exchange rate constants, T=100 K

4. METHODOLOGY OF MEASUREMENTS

4.1. Leading idea

Double Q-switching technique for frequency selective mode of CO laser operation allowed us to study effects of vibration dynamics induced by the first short laser pulse perturbation of VDF on selected vibrational-rotational transition of CO molecule. The second laser pulse on the same transition served as an indicator of relaxation rate of this perturbation. The ratio $\mathbf{Q_2/Q_1=R}$ of the second laser pulse energy to the energy of the first one as a function of the delay time τ_{1-2} was taken as a quantitative measure of VDF recovering.

Measurements of **R** dependencies on τ_{1-2} were carried out for variable experimental conditions: different selected vibrational-rotational transitions; different laser mixture density **N** and temperature **T**; specific input energy (SIE) $\mathbf{Q_{in}}$ deposited into electric discharge; time delay τ_d between beginning of the pump discharge pulse and the first Q-switched laser pulse.

4.2. Description of experimental setup

In the experiments we used cryogenically cooled pulsed electron beam controlled discharge (EBCD) CO laser installation [18] with active volume **V**=2 liters (optical volume $\mathbf{V_{opt}}$=1 liter). The conditions of the experiments were as follows:

- laser gas mixture CO:N_2=1:1;
- laser gas density **N**=0.045-0.070 Amagat;
- initial gas temperature **T**=95-115 K,
- SIE $\mathbf{Q_{in}}$=200-600 J/l.Amagat.

An optical scheme of a laser resonator is presented in Fig. 6. The scheme allowed us to realize very flexible mode of CO laser double-pulse characteristics tuning (including separate and independent spectral line selection and monitoring of temporal behavior of laser radiation intensity by double Q-switching technique). The laser resonator (Fig. 6) consisted of the Q-switching (QS) optical system and spectrally selecting unit separated by the active medium **1**. The laser chamber was sealed by two BaF_2 flat plates **2** inclined at the Brewster angle φ_b with respect to the laser resonator axis.

QS system (see Fig. 6) included totally reflecting mirrors: rotating flat aluminum mirror **3** (rotation speed **V**=0-60000 revolutions/min), concave Au-coated glass mirror **4** ($\mathbf{r_{curv}}$=1.5 m) and flat Au-coated copper mirror **5** with spatial filter **6** which was used to form QS laser pulses duration and

time interval between them. The rotating mirror was placed in the focal plane of the concave mirror **4** ($L=r_{curv}/2$).

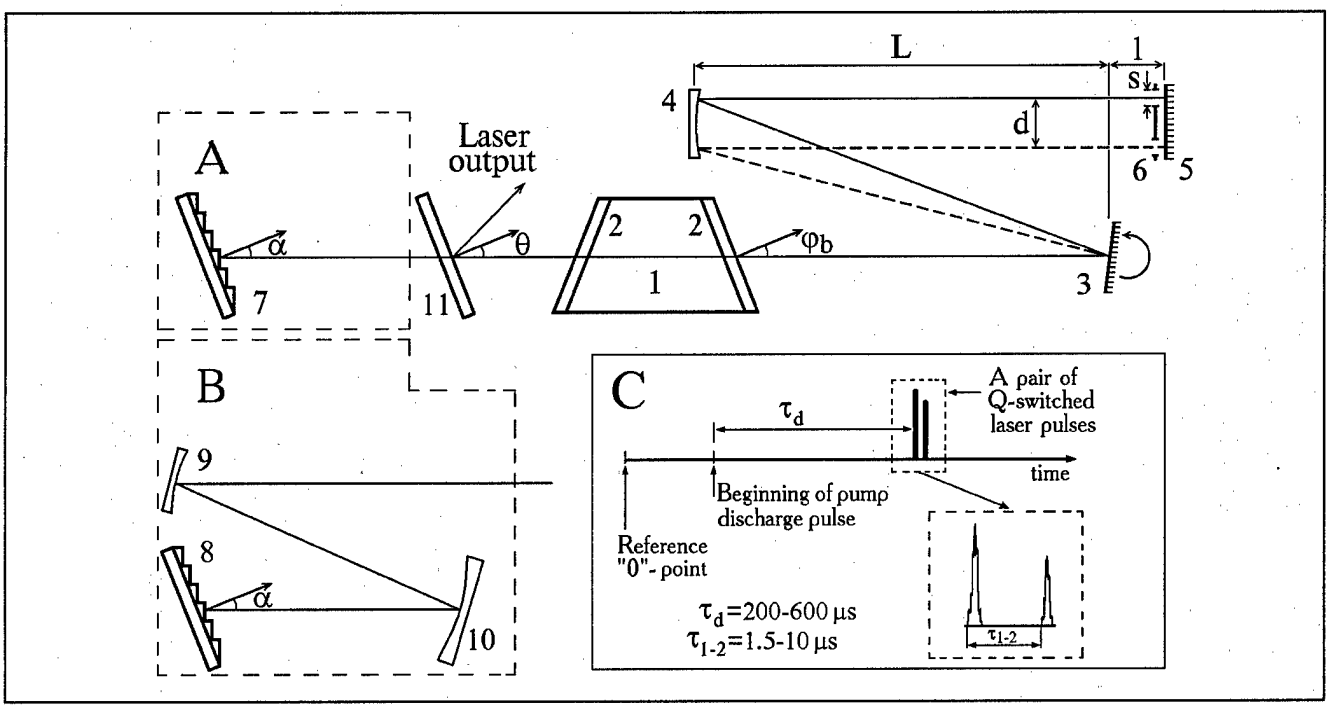

Fig. 6. Optical scheme of frequency selective double Q-switched CO laser. A - spectrally selecting unit exploited in the first series of the experiments (Russian diffraction grating), B - spectrally selecting unit used in the last series of the experiments (US diffraction grating), C - typical time behavior of laser radiation intensity. 1-active medium, 2-Brewster windows, 3-rotating mirror, 4, 9, 10- totally reflecting concave mirrors, 5-totally reflecting flat mirror, 6-spatial filter, 7, 8-diffraction gratings, 11-CaF_2 output flat plate

The flat reflecting mirror **5** was shifted from the focal plane of the mirror **4** at the distance **l~L**/10 to obtain stable configuration of the composite laser resonator. The solid opaque spatial filter **6** had two slits of equal width **S** separated by the distance **d,** which were responsible for the single QS laser pulse duration (τ) and the time delay (τ_{1-2}) between the first and the second QS laser pulses, respectively. We could vary the temporal parameters of double pulse QS CO laser by changing the values of **V**, **S** and **d**: laser resonator QS on-/off- time $\tau_{on/off}$, single QS pulse time duration τ and time delay τ_{1-2} between the first and the second QS laser pulses. In our experiments $\tau_{on/off}$ and τ were fixed at the values of 0.2 μs and 1 μs respectively. Independently, using special electronic delay device, we could change time delay τ_d between the beginning of pump discharge pulse (pump pulse duration ~40 μs) and the first Q-switched laser pulse within the range of 200-650 μs.

Spectrally selecting unit in the laser resonator in the first experimental series (see Interim Reports #1 and #2) consisted of the aluminum diffraction grating **7** (150 grooves per mm, blazing at

32°) made in Russia (Fig. 6, A). The grating was used in Littrow configuration, spectral resolution being of ~2500. The laser spectrum monitoring angle α was controlled with an accuracy of ~0.2%.

In the last experiments we used Al-coated glass diffraction grating **8** (150 grooves per mm, blazing at 26°45') made in USA with additional intracavity telescopic beam expander consisted of concave Au-coated glass mirrors **9** ($\mathbf{r_{curv}}$=0.5 m) and **10** ($\mathbf{r_{curv}}$=1.0 m) - see Fig. 6, B. In this scheme we increased spectral resolution of spectrally selecting unit of the laser resonator up to ~5000 (about two times higher as compared to the scheme A).

The laser output (both in the scheme A and B) was effected by Fresnel reflection of intracavity radiation from the flat CaF_2 plate **11** placed into the laser resonator at the small angle (θ=7°) to its optical axis.

The CO laser output detecting system (which is not presented in Fig. 6) consisted of the IR detector with a response time of ~10^{-9} s, thermoelectric calorimeter with a sensitivity limit of ~10^{-3}J and IR spectrograph with a spectral resolution of ~0.5 cm^{-1} within the wavelength range of 4.5-6.5 μm.

4.3. Experimental procedure of measurements

Typical time behavior of laser radiation intensity (double Q-switching mode of CO laser operation) is presented in Fig. 6, part C.

In all our experiments we measured the ratio $\mathbf{R=Q_2/Q_1}$ as a function of $\tau_{1\text{-}2}$ for selected vibrational-rotational transition, other lasing parameters (τ_d, $\mathbf{Q_{in}}$, **T**, **N**) being fixed. Typical experimental waveforms of laser pulse pair depending on $\tau_{1\text{-}2}$ for laser transition 16→15P(16) are presented in Fig. 7.

High frequency modulation of the laser pulse (see Fig. 7, insertion A) is caused by longitudinal modes beating. A period of the modulation equaled ~50 ns and corresponded to the round-trip time of the laser resonator (laser resonator length ~7.5 m).

It was very important to know as accurately as possible the actual value of laser resonator round-trip optical losses for a comparison of theoretical calculations with experimental data. For this purpose we measured directly the reflection coefficients of all the laser cavity optical elements within the wavelength interval of 5.0-6.2 μm (Fig. 8). The procedure of the round-trip optical losses measurements consisted of the following steps:

1. CaF_2 flat test plate was placed into the laser resonator between its spectrally selecting units A and B and the output plate 11 (see Fig. 6).

2. The energy of CO laser radiation reflected by the plate in both directions was measured by two calorimeters (Fig. 8a).

3. The scheme of measuring the ratio of the two energies was calibrated by substituting of spectrally selecting units by the totally reflecting high quality plane mirror (Fig. 8a).

4. The same procedure was performed for the Q-switching (QS) optical system of the laser resonator (Fig. 8b) by placing the CaF_2 plane plate between the rotating mirror **3** and right side Brewster window **2** (see Fig. 6).

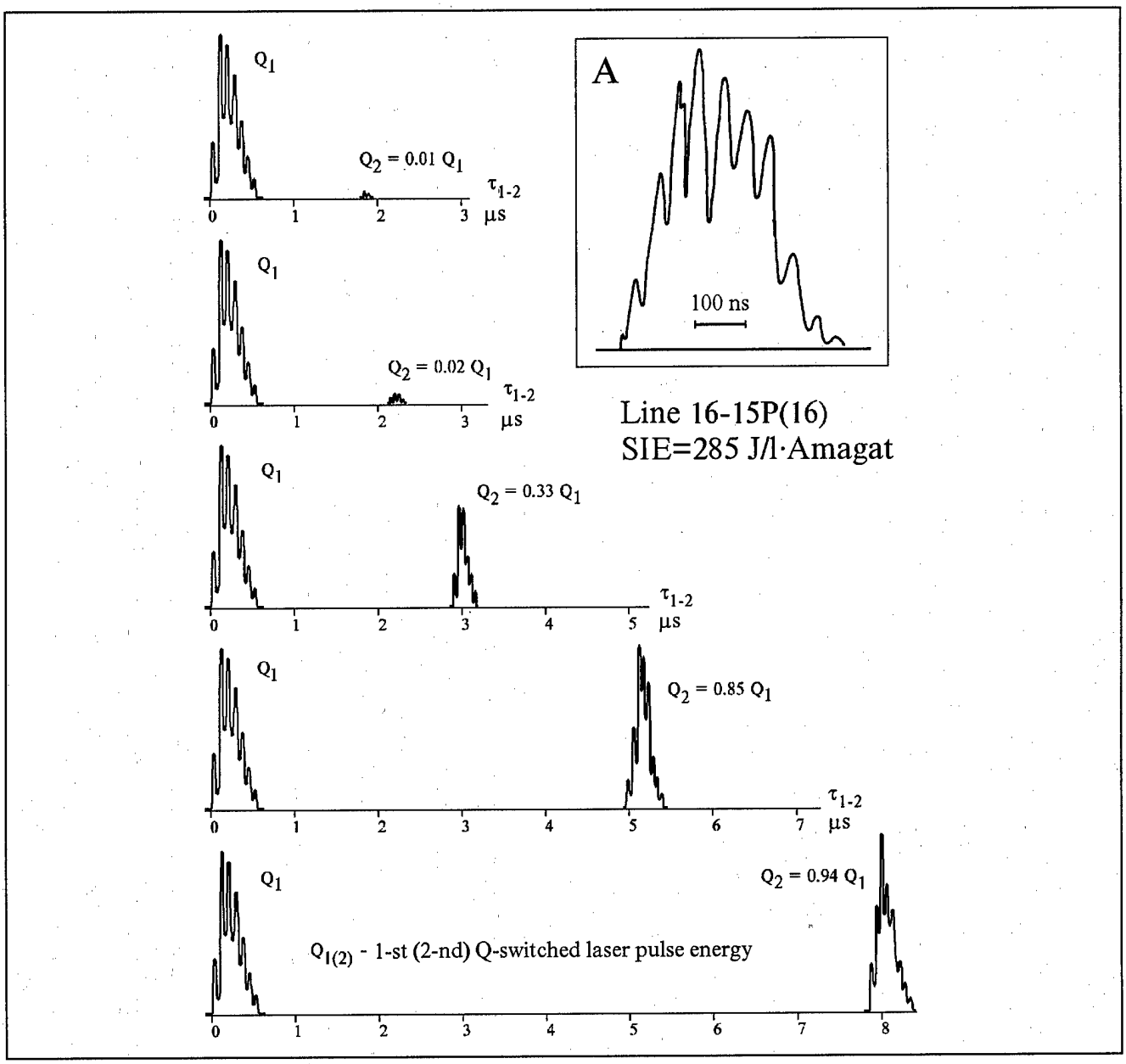

Fig. 7. Typical experimental waveforms of laser pulse pair depending on $\tau_{1\text{-}2}$. Spectral line 16→ 15P(16), SIE=285 J/l Amagat. An insertion A shows the first laser pulse with a high resolution

Using this technique we have found the total round-trip losses of the laser resonator with spectrally selecting unit A (see Fig. 6) based on Russian diffraction grating and used in the first series of the experiments. Total round-trip losses calculated from the experimental data (taking into account a double-path value of outcoupling plate reflection losses) are presented in Fig. 9 (solid curve) as a function of the laser wavelength.

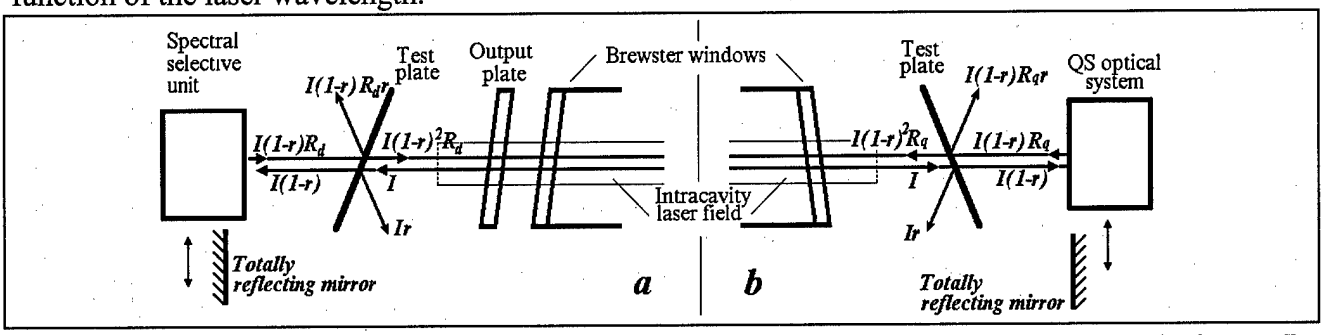

Fig. 8. Spectrally selecting unit (a) and QS optical system (b) optical losses measurements scheme. I - relative intracavity laser field intensity (in one direction), r - reflection coefficient of the test CaF_2 plate, R_d - spectrally selecting unit reflection coefficient, R_q - QS optical system reflection coefficient.

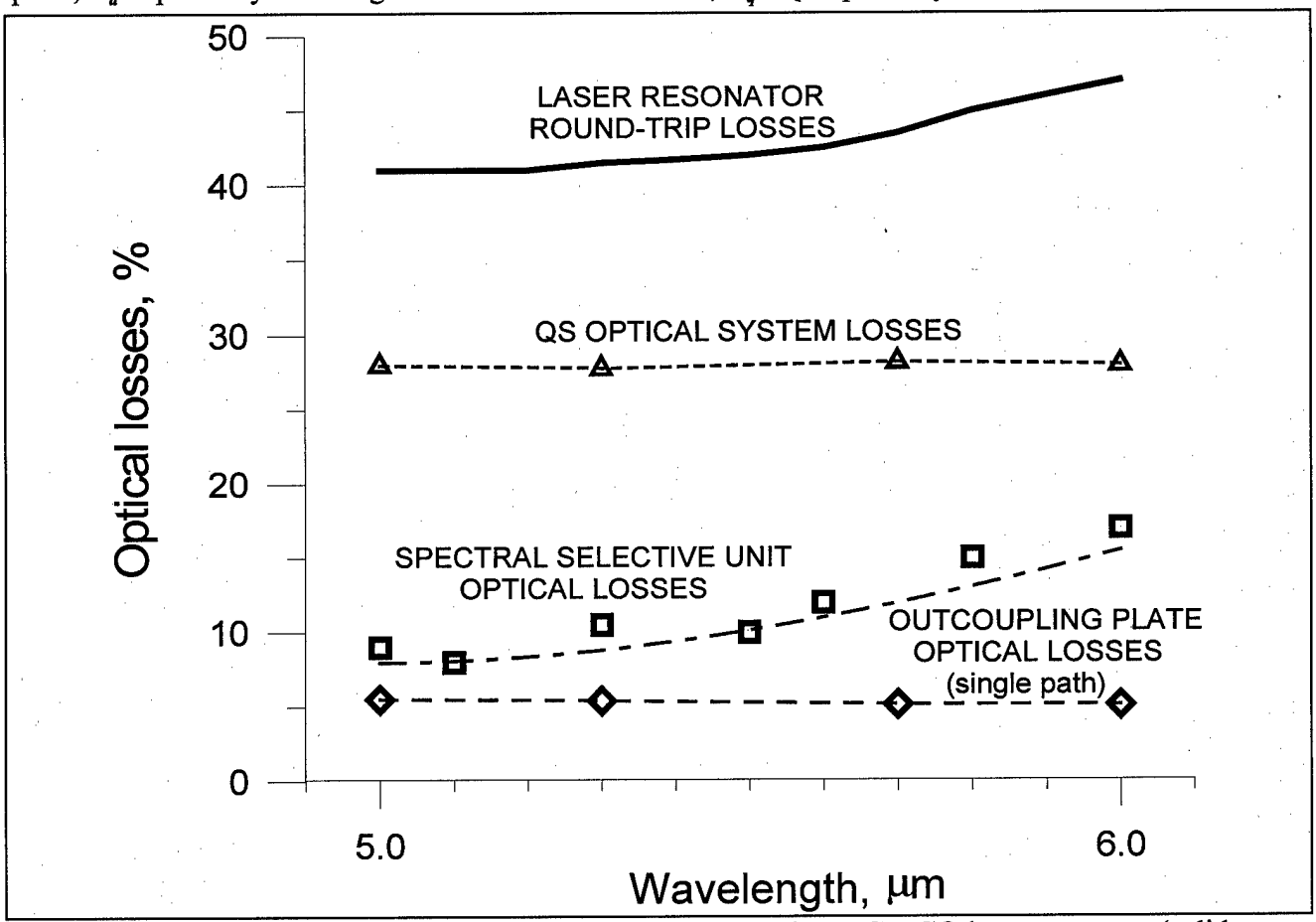

Fig. 9. Wavelength dependencies of: round-trip optical losses in EBCD CO laser resonator (solid curve); QS optical system optical losses (triangular markers); spectrally selecting unit A (see Fig. 6) optical losses (square markers); outcoupling plate single path optical losses (rhombic markers). (The first series of the experiments.)

4.4. Choosing rotational components of CO laser spectrum

For each investigated vibrational band we studied only some vibrational-rotational transitions which were chosen taking into account two criteria:

1. The wavelength difference between selected laser line center and the closest spectral lines of upper and lower adjacent vibrational bands should be ~0.8cm^{-1} or higher (for more stable single line operation of the laser);
2. The selected laser line should coincide with local "transparency window" of atmospheric air and have minimal absorption by water vapor (for decreasing uncontrolled optical losses inside the laser resonator).

4.5. Limitations of the methodology

Delay time τ_d and SIE Q_{in}:

To specify a procedure of the measurements and a definition of the values of τ_d and $\mathbf{Q}_{in}$ we obtained experimentally the dependencies of peak intensity of a single Q-switched laser pulse on time delay τ_d for different specific input energies $\mathbf{Q}_{in}$ (Fig. 10). Believing that easier tractable and more reproducible are data obtained for conditions when the VDF evolution proceeds in a quasi-stationary manner in the range of vibrational levels involved into lasing, parameters τ_d and $\mathbf{Q}_{in}$ were chosen within 350-600 μs and 270-400J/l.Amagat intervals, respectively.

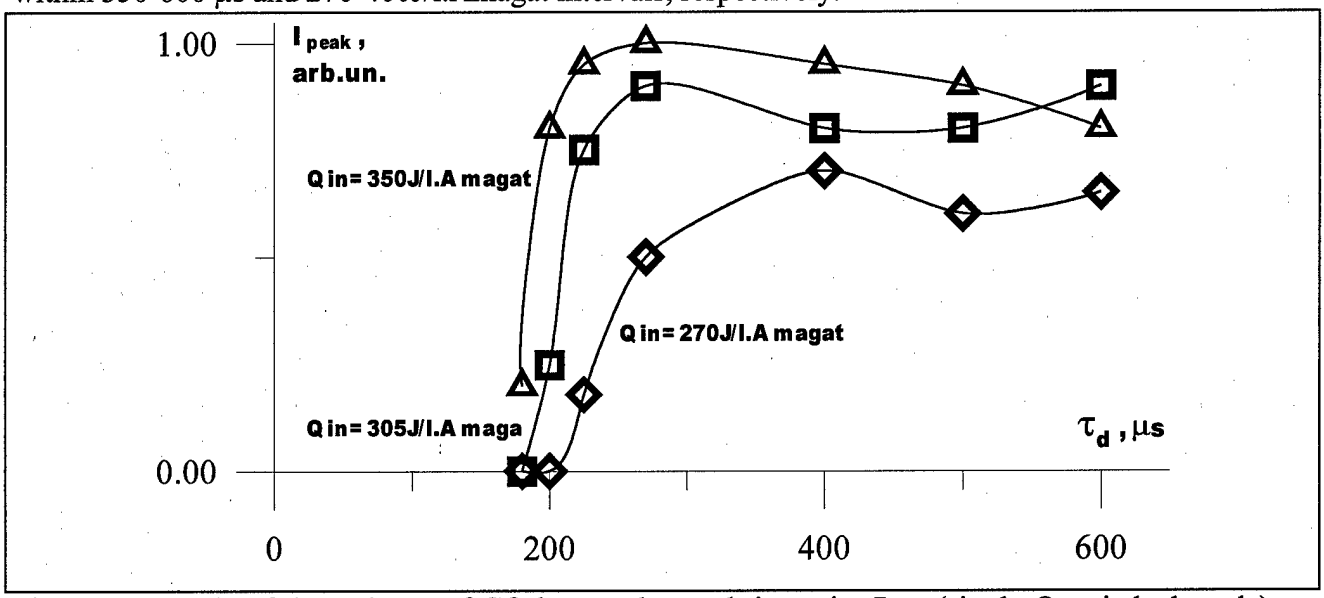

Fig. 10. Example of dependence of CO laser pulse peak intensity $\mathbf{I}_{peak}$ (single Q-switched mode) on time delay τ_d for different SIE $\mathbf{Q}_{in}$. Spectral line 18→17 P(18).

This procedure was executed for each selected laser transition for definition of suitable values of both τ_d and $\mathbf{Q}_{in}$.

Spectral selectivity of laser resonator

In the first series of the experiments we used the spectrally selecting unit A of the laser resonator (see Fig. 6) with total spectral resolution ~2500. The laser action was obtained for double Q-switched mode of CO laser operation on a lot of vibrational-rotational transitions up to the vibrational band 33→32. But in the most cases spectral resolution of the spectrally selecting unit A (~0.7cm^{-1}) did not permit us to achieve reliably single line CO laser operation. It seems to be associated with a strong overlapping of selected line and wings of spectral lines belonging to adjacent vibrational bands. In the experiments this fact was confirmed by very complex time behavior of Q-switched CO laser pulse intensity (Fig. 11).

The waveforms similar to ones presented in Fig. 11 were observed most often, if we studied laser transitions on higher vibrational bands. It happened because, due to respectively high round-trip optical losses, we had to compensate a decrease of small signal gain on higher levels by an increase of the SIE. Multi-peak time structure of single Q-switched laser pulse appeared, which corresponded to multi-frequency lasing, and in the most cases we were unable to separate it using spectrally selecting unit A of the laser resonator (see Fig. 6).

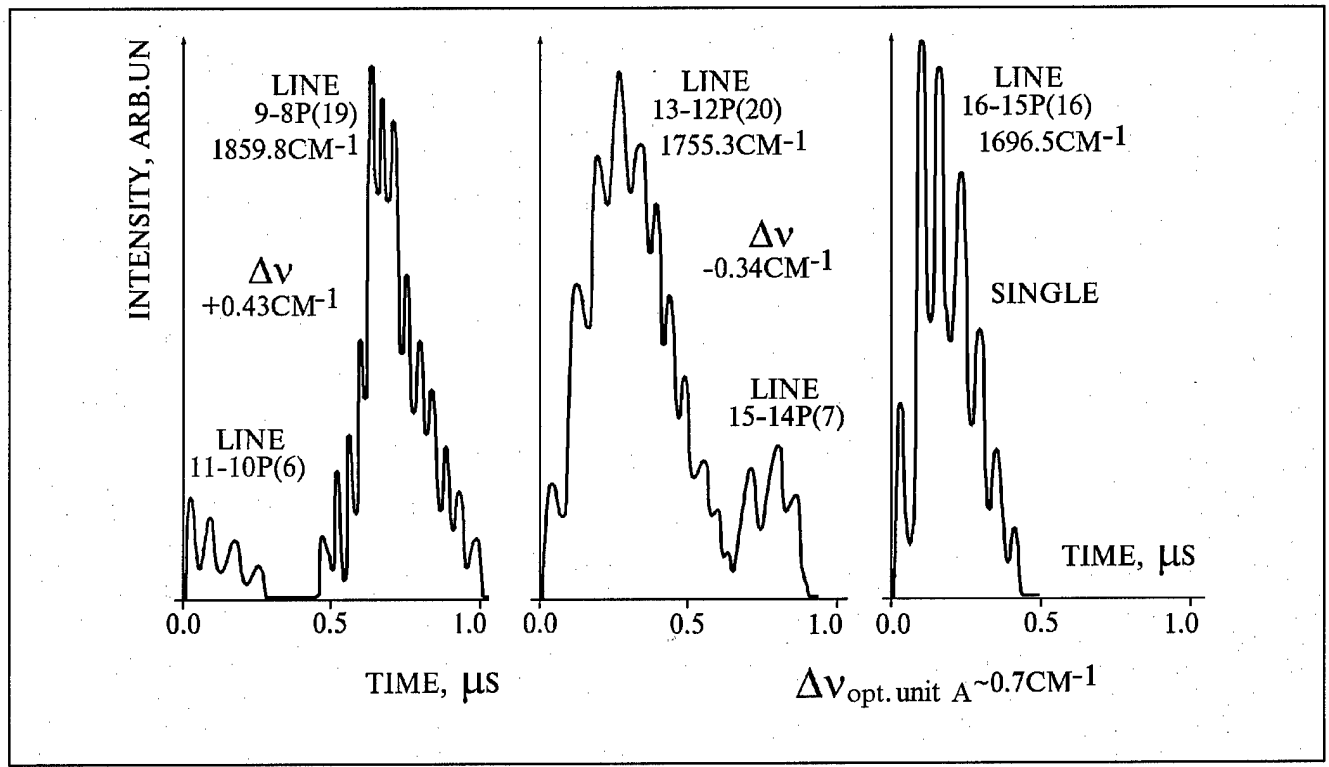

Fig. 11. Examples of single Q-switched CO laser pulse intensity waveforms. Multi (double) frequency (left and center) and single frequency (right) lasing mode.

Another manifestation of the described effects one can see in Figs. 12 and 13, where the $\mathbf{R}=\mathbf{Q_2}/\mathbf{Q_1}$ dependencies on $\tau_{1\text{-}2}$ are presented for single- and multi-frequency operation of the laser with double pulse Q-switching, respectively.

In case of single frequency lasing (Fig. 12) for any SIE we observed smooth curves corresponding to a recovering process of the vibrational distribution function and, hence, to an increase of laser pulse energy on selected transition. Unfortunately, such a regular behaviour of **R** was observed only for three vibrational-rotational transitions, where experimental data can be compared with theoretical calculations for different SIE. These transitions were: 7→6P(16), 16→15P(16) and 18 →17P(18).

For a great number of laser transitions (~12 lines) we observed only the pictures analogous to ones presented in Fig. 13. These experimental data appeared to be inappropriate for comparing with theoretical calculations.

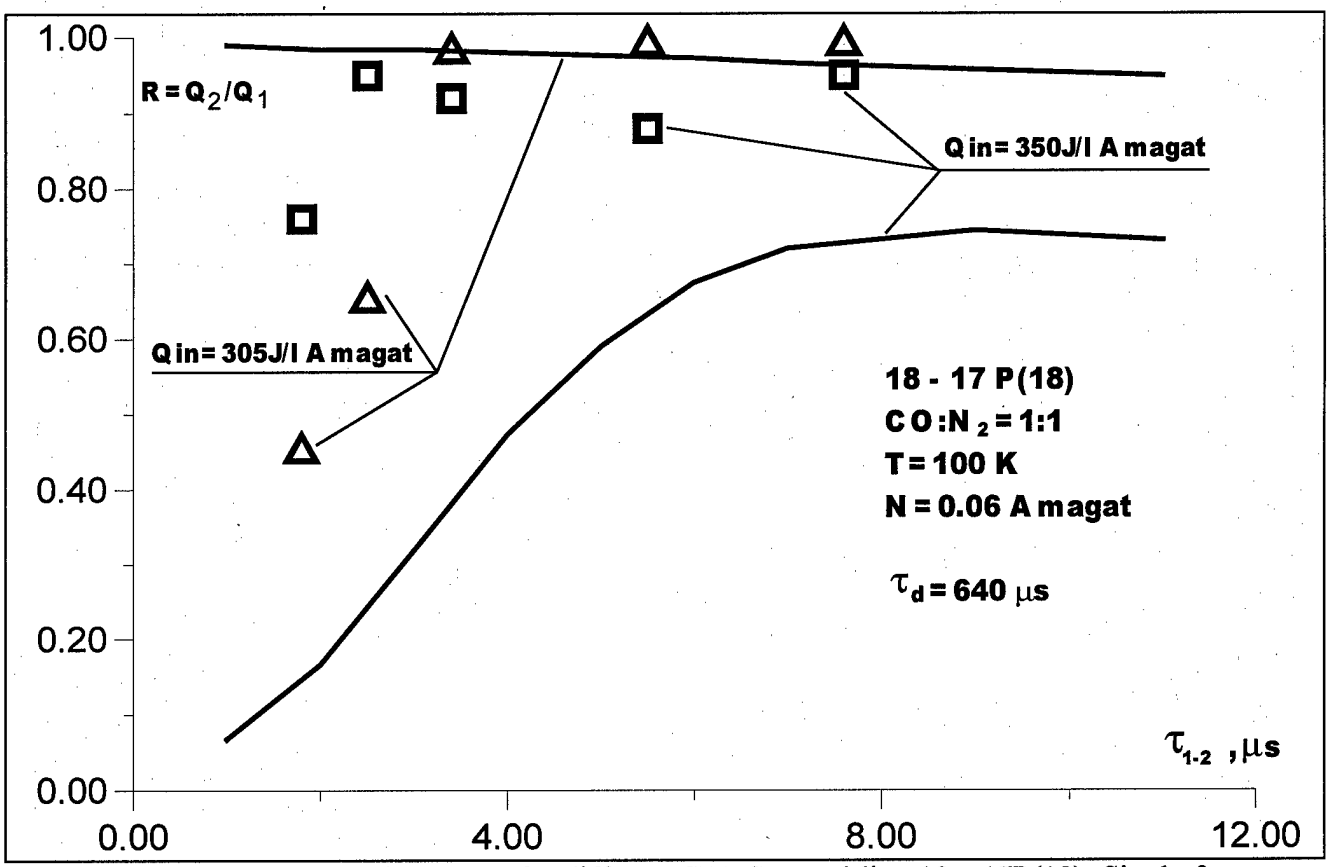

Fig. 12. $\mathbf{R}=\mathbf{Q_2}/\mathbf{Q_1}$ dependencies on $\tau_{1\text{-}2}$ for different SIE. Spectral line 18→17P(18). Single frequency lasing mode (theory and experiments).

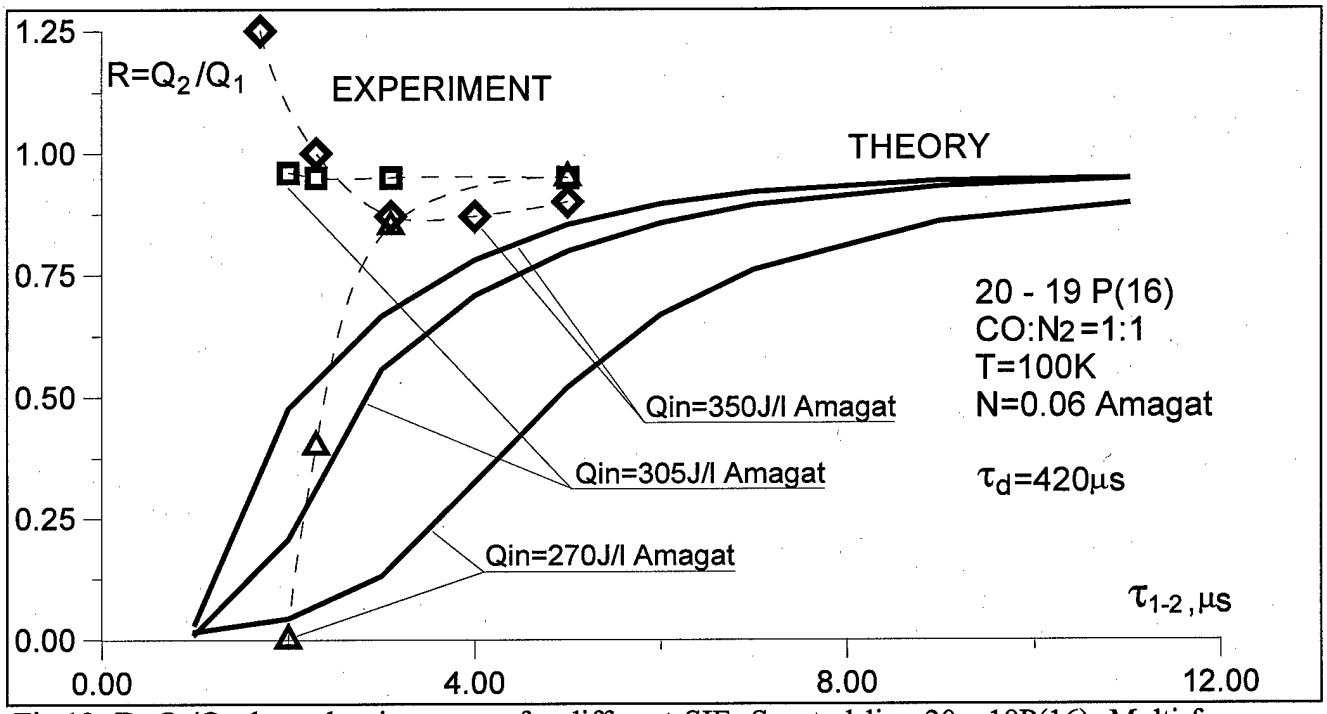

Fig.13. $\mathbf{R=Q_2/Q_1}$ dependencies on $\tau_{1\text{-}2}$ for different SIE. Spectral line 20→19P(16). Multi-frequency lasing (theory and experiment).

For these reasons the last series of the experiments were carried out by using spectrally selecting unit B of the laser resonator (see Fig. 6) based on the US diffraction grating of higher reflectivity with additional intracavity beam expander. This scheme ensured the spectral resolution of the laser resonator ~5000 (spectral resolution ~0.35cm^{-1}) and allowed us to obtain experimentally reliable single line lasing data on 6 transitions: 8→7P(10), 9→8P(11), 13→12P(11), 15→14P(13), 19 →18P(15) and 20→19P(14).

Round-trip losses of the laser resonator

In spite of higher reflectivity of US diffraction grating (with respect to Russian one), adding two-mirror beam expander into the laser cavity did not allow us to decrease significantly total round-trip losses of the laser resonator having spectrally selecting unit B (see Fig. 6). They were about the same ones as for the laser resonator based on spectrally selecting unit A (~40-50%). For this reason, we could not carry out the reliable experiments on laser transitions higher than **v**→**v**-1~20→19, which are more desirable for comparing with theoretical calculations because of expected stronger effects of multi-quantum V-V exchange and for achieving deeper understanding energy exchange processes in CO laser active medium (especially on highly excited vibrational levels **v**~30-40, where the first-overtone CO laser operates).

It should be noted that the laser resonator consisted of a lot of reflecting optical elements (see Fig. 6 with unit B) and had high total round-trip losses. The diffraction grating and all the mirrors (except rotating one) available now have the highest reflectivity. Only aluminum rotating mirror has total reflectivity ~90% and, being passed two times during the round -trip of the resonator, contributed significantly to the round-trip optical losses (~20%). A substitution of this mirror by, for example, Au-coated one (not available now) is the simplest way to decrease optical losses and get the possibility to study experimentally laser transitions $v \rightarrow v\text{-}1 \sim 25 \rightarrow 24$ and higher.

Threshold properties of the laser resonator

Because of proximity to threshold lasing in our laser scheme, a reproducibility of the experimental data was not very good (particularly, at the shortest delay time $\tau_{1\text{-}2} < 2$ μs) and a statistical error might reach up to ~50% in some cases. This methodical disadvantage, which can not be removed at the moment, decreased significantly an accuracy of a comparison of the experimental data with theoretical calculations. Excluding a possibility of replacing one of the mirrors to the mirror with higher reflectivity, the second way to improve the situation is the use of master oscillator - laser amplifier technique for measuring experimentally the VDF recovering time perturbed by radiation on selected vibrational-rotational transitions. By using master oscillator-laser amplifier scheme, we can get rid of threshold effects and achieve higher accuracy of measurements.

5. RESULTS AND DISCUSSION

5.1 Theoretical description of Q-switching process

In the theoretical model, Q-switching process was approximated using time dependence of cavity threshold gain shown in Fig. 14. The threshold gain for the blocked resonator was taken high enough to avoid lasing on the transitions studied. The lowest value of the threshold gain was taken close to the measured in this report value (see Section 4.4), and depended on the laser wavelength. A duration of single Q-switching process was 1 μs.

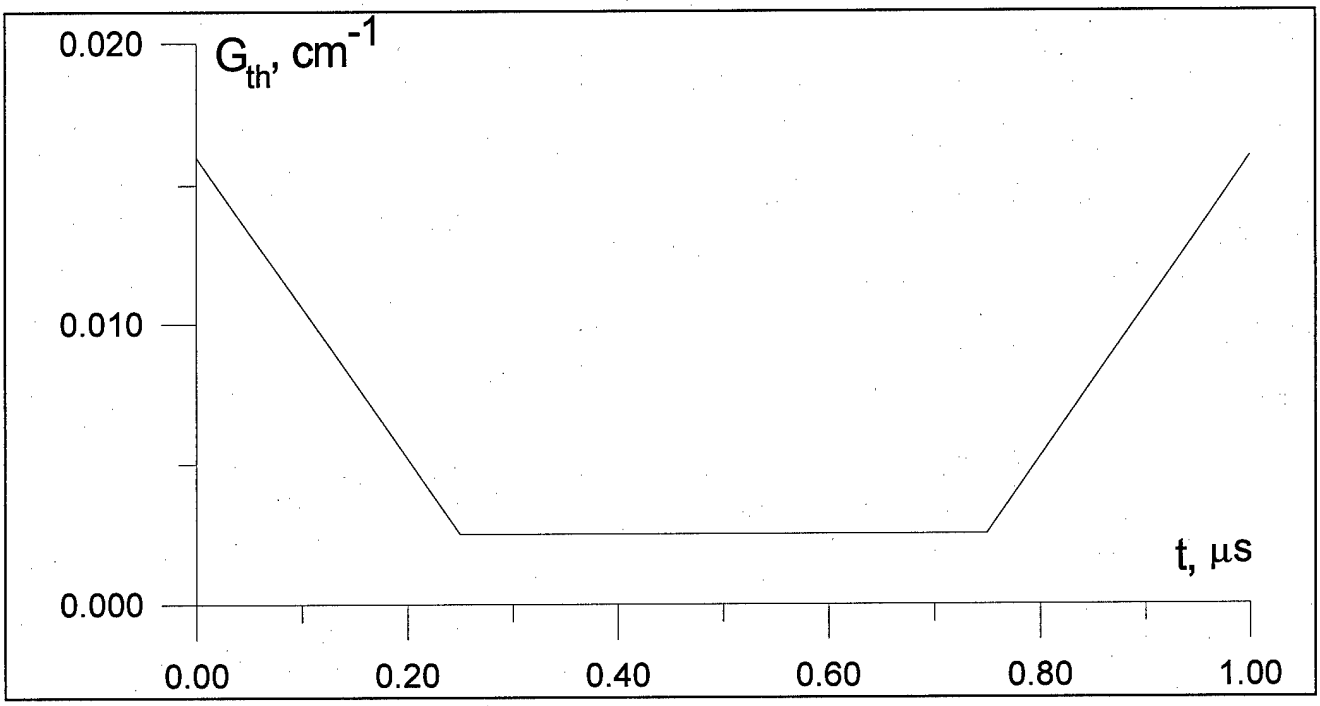

Fig. 14. Time behavior of laser resonator Q-switching used in the calculations.

When using double Q-switching technique described below, either energy or peak intensity of two consequent pulses can be considered as a quantitative measure of recovering VDF shape. From theoretical point of view any quantity might be equally informative. However, in the experiments, pulse waveforms were complicated and not reproduced quite well. Therefore, energies of the two pulses were compared and served as an indicator of the VDF recovering. If the cavity threshold gain was high, laser pulse was of low intensity, and as a result, population of vibrational levels was disturbed only slightly by lasing process. In this case, the methodology was not informative. Therefore, the laser lines coincident with water vapor absorption lines were excluded from comparison procedure.

5.2. Comparison of SQE and MQE models in analysis of double pulse Q-switched CO laser.

To compare results produced by SQE and MQE models, calculations were made using the traditional SQE model with rate constants from [11]. The results of the calculations of energy recovering curve, that is dependencies on delay time of the ratio $\mathbf{R=Q_2/Q_1}$ of energy in the second CO laser pulse to the energy in the first one for two consequent laser pulses on transitions in vibrational bands $v \rightarrow v\text{-}1=7 \rightarrow 6$ and $16 \rightarrow 15$ are presented in Figs. 15a and 15b, respectively, together with the results of the experimental measurements. Squared markers show the results of the measurements. One

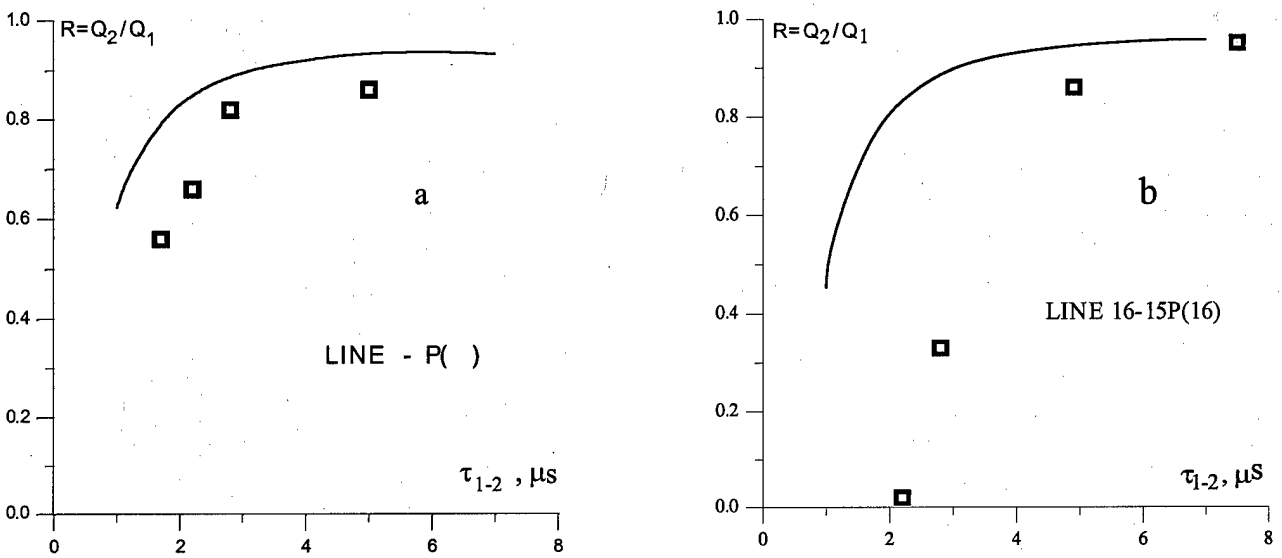

Fig. 15. Energy recovering calculations (curves) and experimental results (markers) versus time delay $\tau_{1\text{-}2}$ for laser transitions $7 \rightarrow 6P(16)$ - (a) and $16 \rightarrow 15P(16)$ - (b), specific input energy 285 J/l.Amagat.

can easily see that the measurements and calculations demonstrate a good agreement for lower transition and differ considerably for higher one for short delays. That is, the rate of gain recovering on high vibrational levels $v>14\text{-}15$ in the experiments was much slower than predicted one. This fact shows that the commonly used SQE model fails to describe VDF dynamics for these high levels.

Additional evidences on differences in SQE and MQE models were obtained in calculations of laser pulse forms and recovering curves for rotational transition J=16 in vibrational band $v=25 \rightarrow 24$. Selected rotational line was near a maximum of laser gain for this vibrational band. Fig. 16 demonstrates the corresponding energy recovering curves for the two models. Fig. 17 shows the

results of calculations of laser radiation temporal behavior for double pulse Q-switched CO laser obtained by using SQE (Fig.17a) and MQE models (Fig. 17b). Delay time between the pulses is 2 μs.

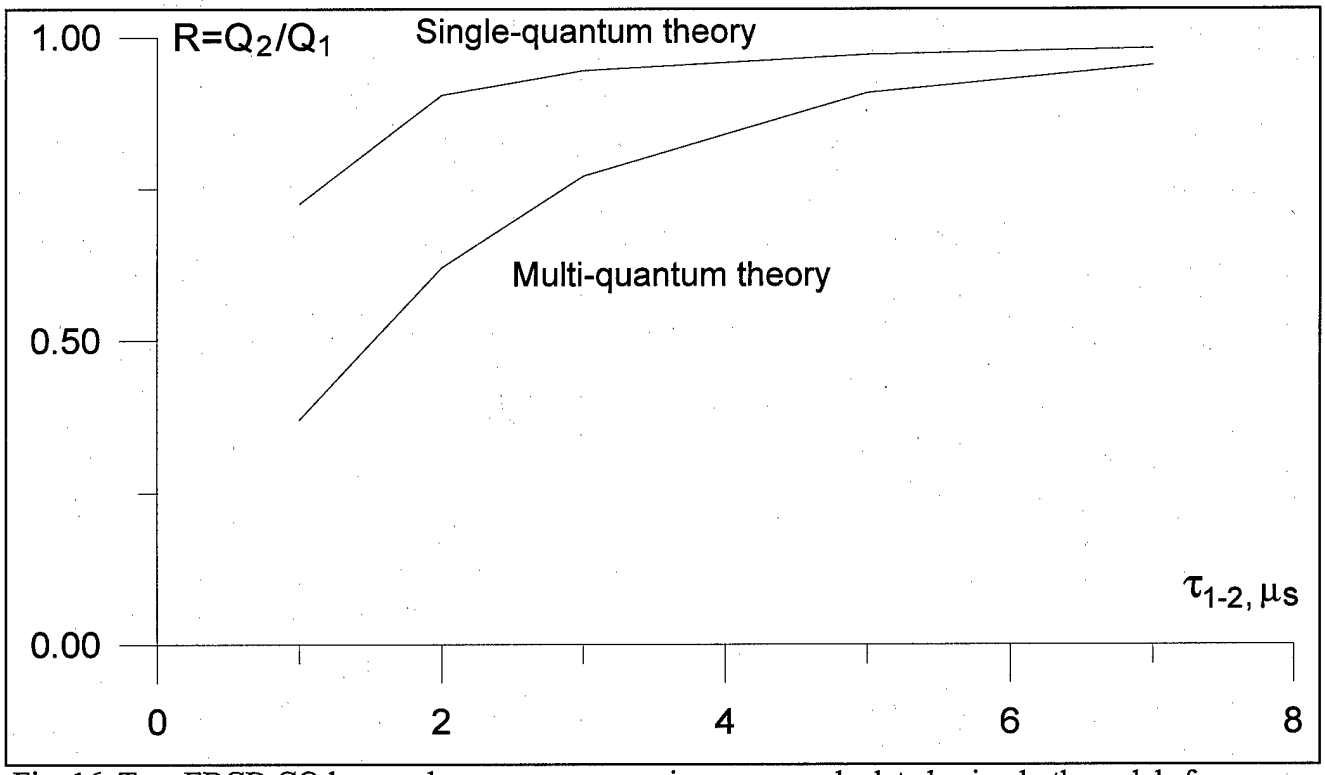

Fig. 16. Two EBCD CO laser pulses energy recovering curves calculated using both models for spectral line 25→24P(16).

One can see a considerable difference in the results for the two models. Energy recovering proceeds slower for the multi-quantum model. Also the pulse waveforms differ strongly. One should mention also that the energy of the first pulse is about 1.5 times higher than calculated by using SQE model. This result is very important for the description of single line selective mode of CO laser operation. As one could expect, SQE model overestimates considerably laser pulse energy for the selective mode of CO laser operation.

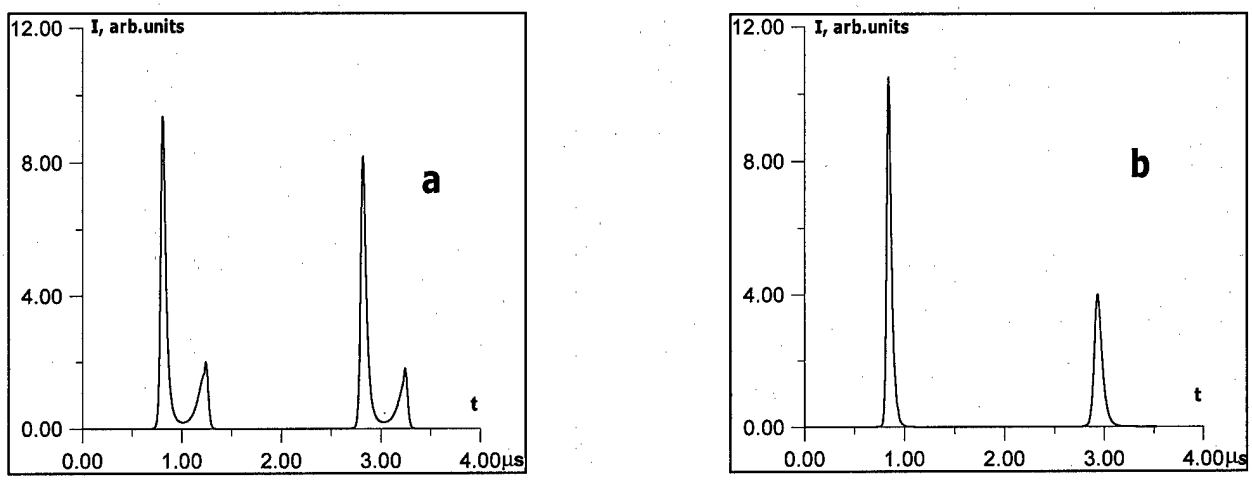

Fig. 17. QS CO laser pulse waveforms calculated using SQE (a) and MQE (b) models.

5.3. Double Q-switching mode of CO laser operation (fundamental band lasing)

As it was mentioned above, two series of experiments were performed with different optical schemes of spectrally selecting units, the first one based on the Russian grating, and the second based on the grating manufactured in the US and with a beam expander. The Table 3 summarizes the experimental data obtained. The experimental conditions are also described in this Table. It is worth to note that gas mixture composition and the pump energy are quite different for excitation of lasing on lower and higher than 16→15 transitions.

Table 3. Total list of investigated CO laser transitions and corresponding experimental conditions.

V→V-1	P(J)	λ, μm	Q_{in}, J/l.Amagat	τ_d, μs	Spectral unit	Mixture, CO:N_2
5→4	P(16)	5.064	285	330	A	1:6
6→5	P(16)	5.131	285	330	A	1:6
7→6	P(16)	5.199	285	330	A	1:6
8→7	P(16)	5.270	285	330	A	1:6
9→8	P(11)	5.285	250	350	B	1:1
9→8	P(19)	5.377	285	330	A	1:6
11→10	P(16)	5.490	285	330	A	1:6
12→11	P(16)	5.667	285	330	A	1:6
13→12	P(11)	5.586	250; 290	590	B	1:1
13→12	P(20)	5.697	285	330	A	1:6
14→13	P(16)	5.726	285	330	A	1:6
15→14	P(13)	5.770	335; 375	590	B	1:1
15→14	P(15)	5.796	285	330	A	1:6
16→15	P(16)	5.895	285	330	A	1:6
17→16	P(15)	5.967	200-400	420, 640	A	1:1
17→16	P(17)	5.996	285	330	A	1:6
18→17	P(18)	6.085	200-400	420, 640	A	1:1
19→18	P(15)	6.149	330	590	B	1:1
20→19	P(13)	6.215	200-400	420, 640	A	1:1
20→19	P(14)	6.229	560	590	B	1:1
23→22	P(15)	6.242	200-400	420, 640	A	1:1
25→24	P(15)	6.756	200-400	420, 640	A	1:1
30→29	P(15)	7.351	200-400	420, 640	A	1:1
33→32	P(13)	7.717	200-400	420, 640	A	1:1

In the first series of the experiments a great scatter in data and irregular behavior of $\mathbf{R}(\tau_{1\text{-}2})$ curves were observed. Figs. 12 and 13 illustrate the situation. A comparison with the results of

calculations presented in these figures demonstrates that a correlation between the theory and the experiment does exist but only for a few cases.

For the transition 18→17P(18) a small signal gain is not much higher than the threshold gain. Therefore, results of the numerical simulations and measurements are quite sensitive to variations of the SIE. As was mentioned above, these data are not informative. In particular, the calculated recovering energy ratio is close to unity being almost independent of delay time at the SIE $\mathbf{Q_{in}}$=305 J/l Amagat. This is explained by a low level of lasing intensity, which produces a negligible perturbation of the VDF. For $\mathbf{Q_{in}}$=350 J/l Amagat the theory predicts a typical relaxation behavior having, however, almost no correlation with the experimental one.

A small signal gain for the transition 20→19P(16) is higher, and one may expect better reproducibility and agreement with the experiment. However, the experimental energy recovering curves for $\mathbf{Q_{in}}$=305 and 350 J/l Amagat demonstrate quite unexpected time behavior. The reason is the problem of single line lasing discussed in Section 4.5. A spectral selectivity of the scheme A in Fig. 6 is not sufficient to suppress lasing on vibrational-rotational transitions belonging to upper and/or lower adjacent vibrational bands. Just lasing on a different transition gave rise to the magnitude of **R** greater than unity for $\mathbf{Q_{in}}$=350 J/l Amagat at $\tau_{1\text{-}2}$=2 μs in Fig. 13.

A replacement of Russian grating to one manufactured in the US would not produce an improvement of the situation by itself. However, lower radiation losses for the latter grating allowed us to introduce a laser beam expander into the optical scheme , which increases a cross-section of the laser beam at the grating. As a result, the spectral selectivity of the system increased, and it became feasible to realize single-wavelength operation in the double Q-switching mode. Experimental data analyzed below were obtained by using this optical scheme.

Theoretically, the recovering energy ratio R was calculated as a function of time delay. The results are presented in Figs. 18-24 in comparison with the experimental data displayed by markers. The theoretical results are depicted by a solid line. Let us remind that for our calculations, just the multi-quantum exchange theory based on rate coefficients for vibration-vibration exchange calculated by Billing was exploited. One can see a reasonably good agreement between the theoretical predictions and experimental measurements.

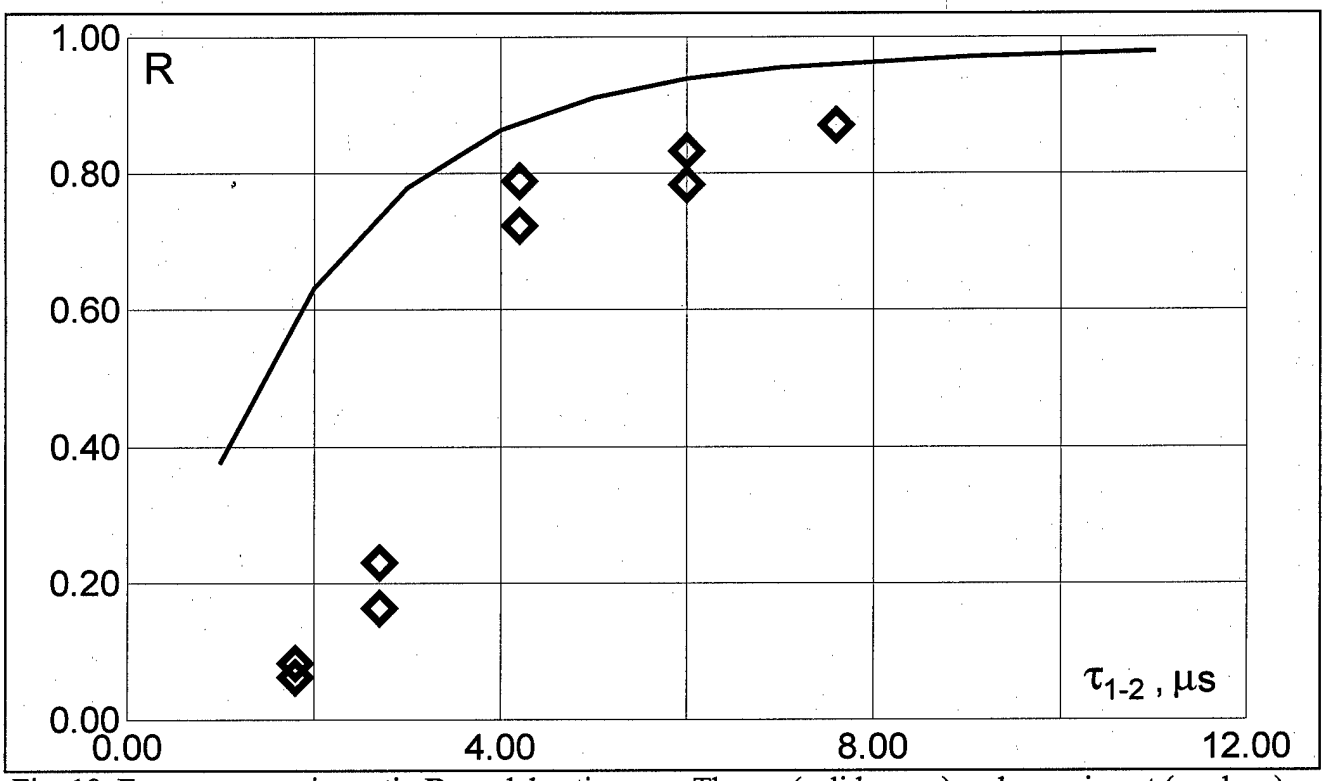

Fig. 18. Energy recovering ratio **R** vs. delay time $\tau_{1\text{-}2}$. Theory (solid curve) and experiment (markers). Spectral line 9→8P(11), $\mathbf{Q}_{in}$=250 J/l Amagat, τ_d=350 μs.

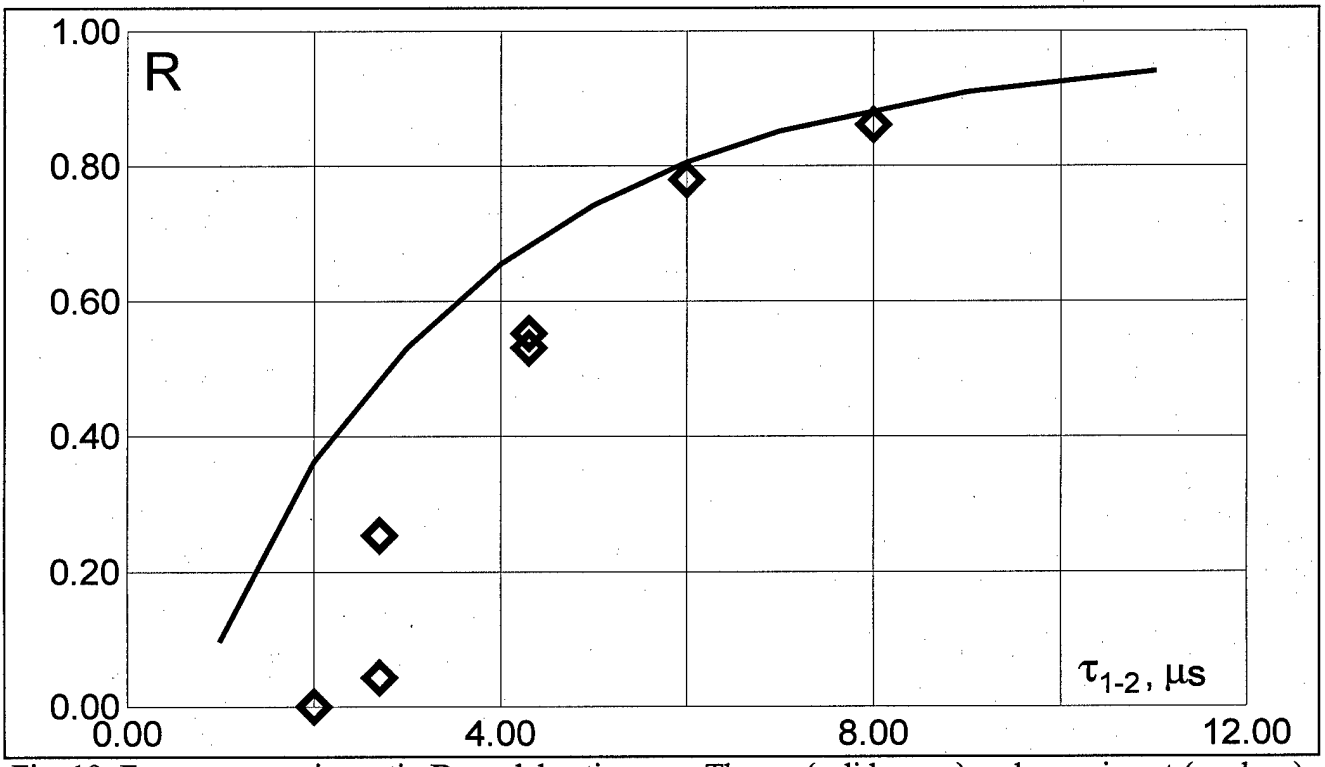

Fig. 19. Energy recovering ratio **R** vs. delay time $\tau_{1\text{-}2}$. Theory (solid curve) and experiment (markers). Spectral line 13→12P(11), $\mathbf{Q}_{in}$=250 J/l Amagat, τ_d=590 μs.

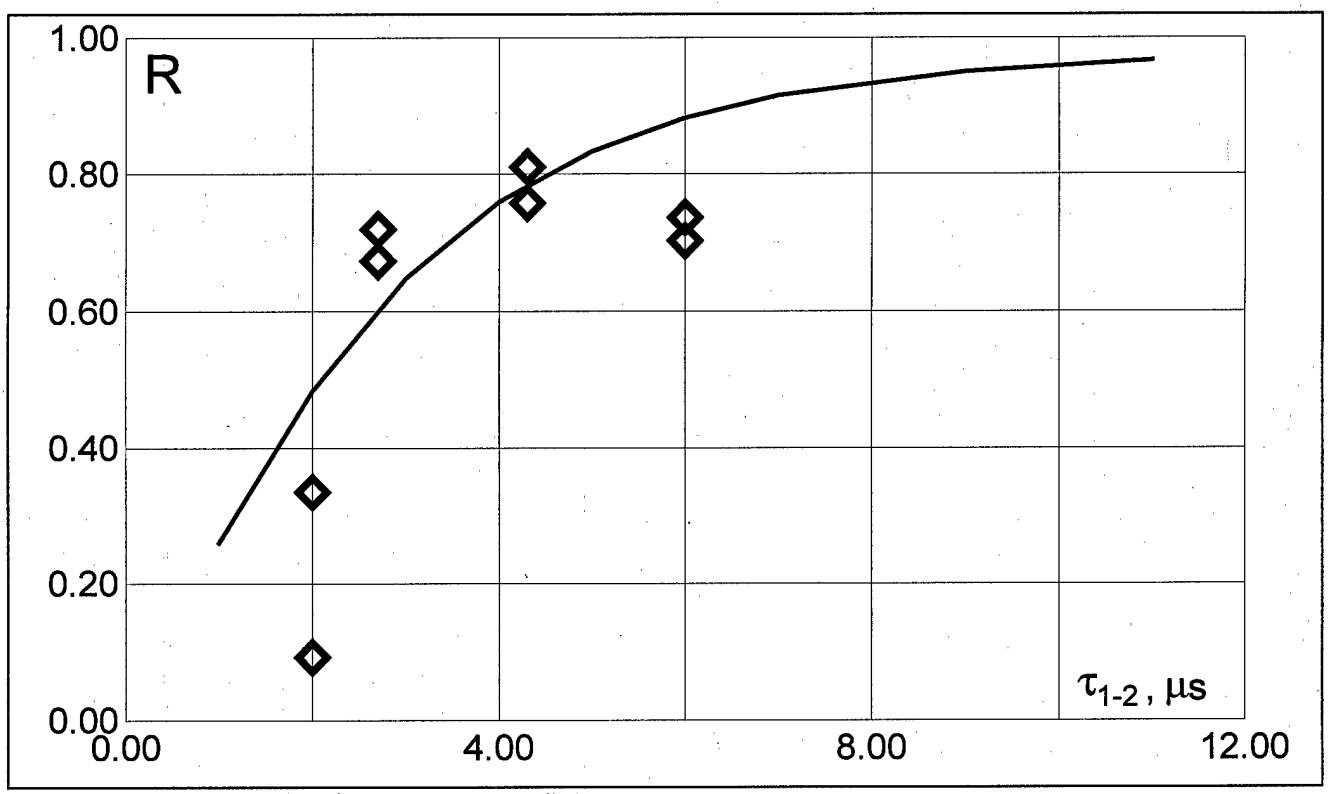

Fig. 20. The same as in Fig.19; $\mathbf{Q_{in}}$=290 J/l Amagat

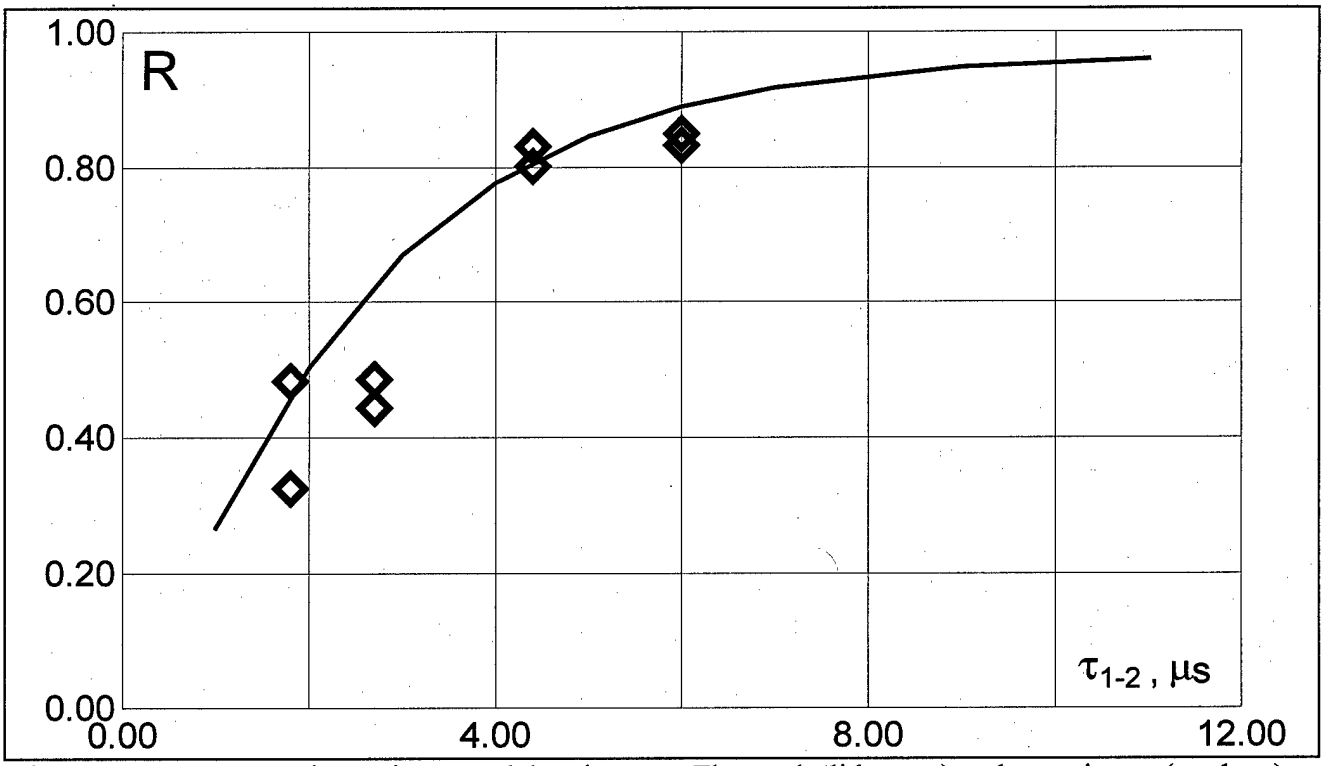

Fig. 21. Energy recovering ratio **R** vs. delay time $\tau_{1\text{-}2}$. Theory (solid curve) and experiment (markers). Spectral line 15→14P(13), $\mathbf{Q_{in}}$=335 J/l Amagat, τ_d=590 μs.

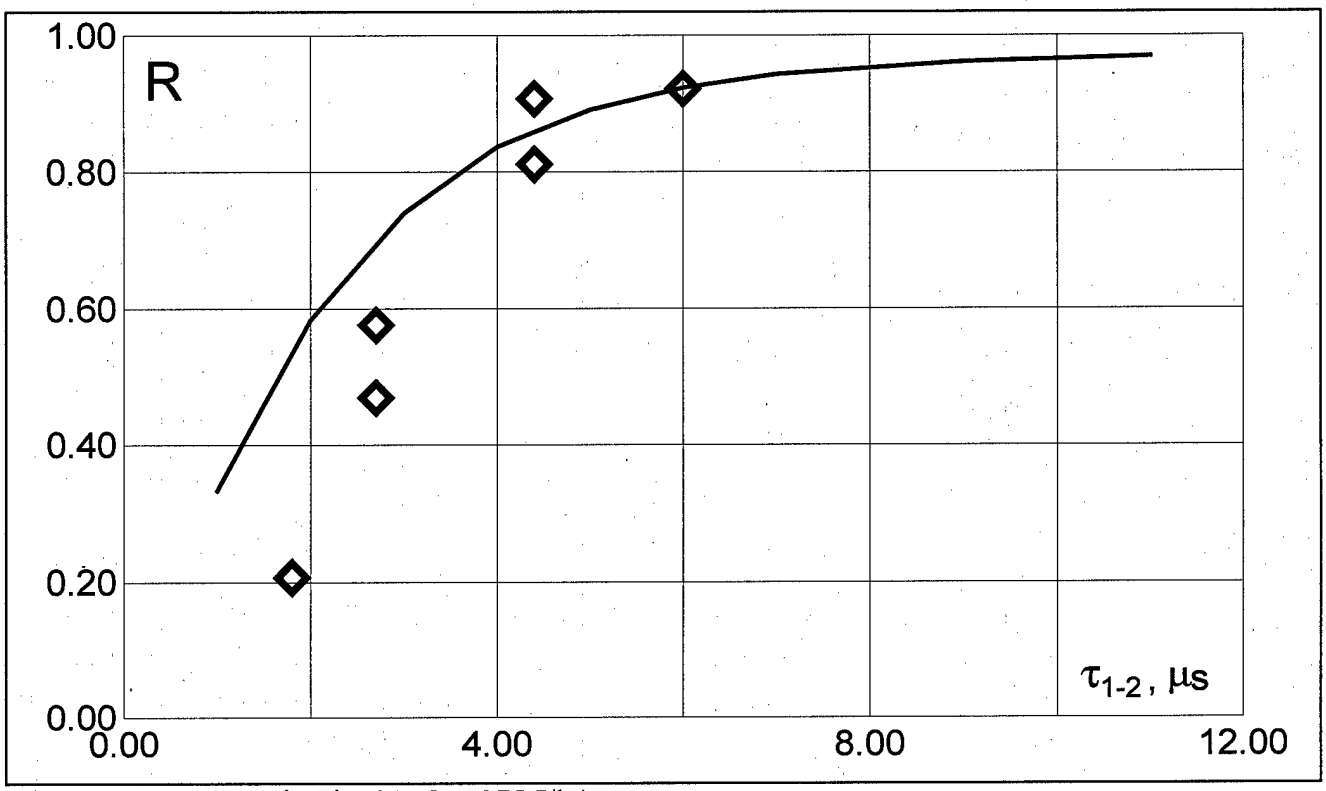

Fig. 22. The same as in Fig. 21; $\mathbf{Q_{in}}$=375 J/l.Amagat

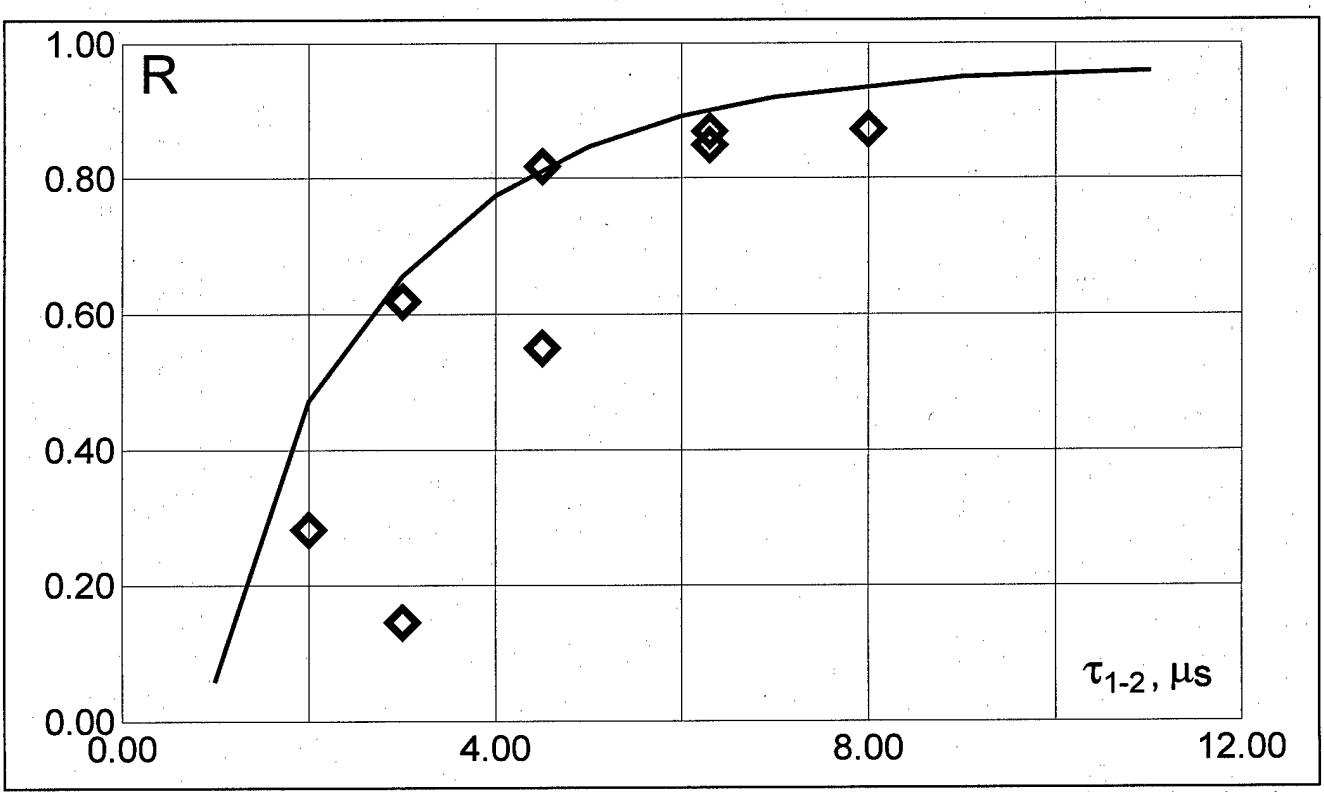

Fig. 23. Energy recovering ratio **R** vs. delay time $\tau_{1\text{-}2}$. Theory (solid curve) and experiment (markers). Spectral line 19→18P(15), $\mathbf{Q_{in}}$=330 J/l Amagat, τ_d=590 μs.

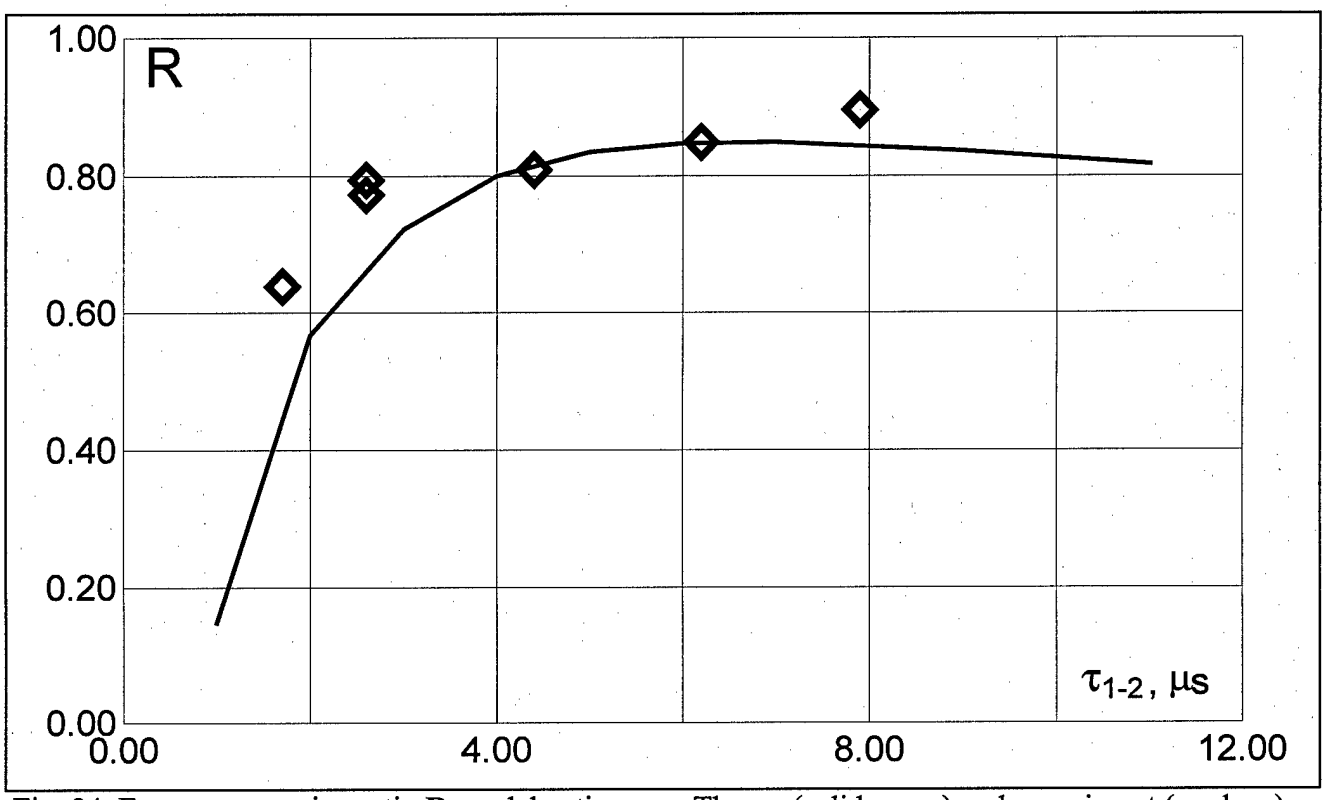

Fig. 24. Energy recovering ratio **R** vs. delay time $\tau_{1\text{-}2}$. Theory (solid curve) and experiment (markers). Spectral line 20→19P(14), $\mathbf{Q}_{in}$=560 J/l Amagat, τ_d=590 μs.

The delay time $\tau_{0.8}$ corresponding to the energy recovering ratio of 0.8 can be taken as a reasonable measure of the process for the given experimental conditions. From Figs. 19-24 it can be seen that both theory and experiment give the values of $\tau_{0.8}$ in the range (4.5-6) μs.

5.4. First-overtone CO laser characteristics.

The observed agreement between theoretical predictions and experimental measurements using double-pulse procedure, particularly being sensitive to details of the V-V energy exchange, encouraged us to apply the same model to a description of characteristics of a first overtone (FO) CO laser. A reason was that this laser operates typically on higher transitions than usually fundamental band CO laser does. Evidently, the multi-quantum effects in vibrational exchange should influence upon a description of FO CO laser characteristics.

In modeling, laser mixture, pump and resonator parameters supposed to be the same as in measurements performed with US grating, namely, SIE=360 J/l Amagat, T=100 K, N=0.12 Amagat. Two threshold gain values - $1.4\cdot10^{-3}$ and 10^{-3} cm^{-1} were considered in calculations. Fig. 25 shows the comparison of these calculations and the measurements. For comparison, Fig. 26 shows also the results obtained earlier within the framework of SQE model.

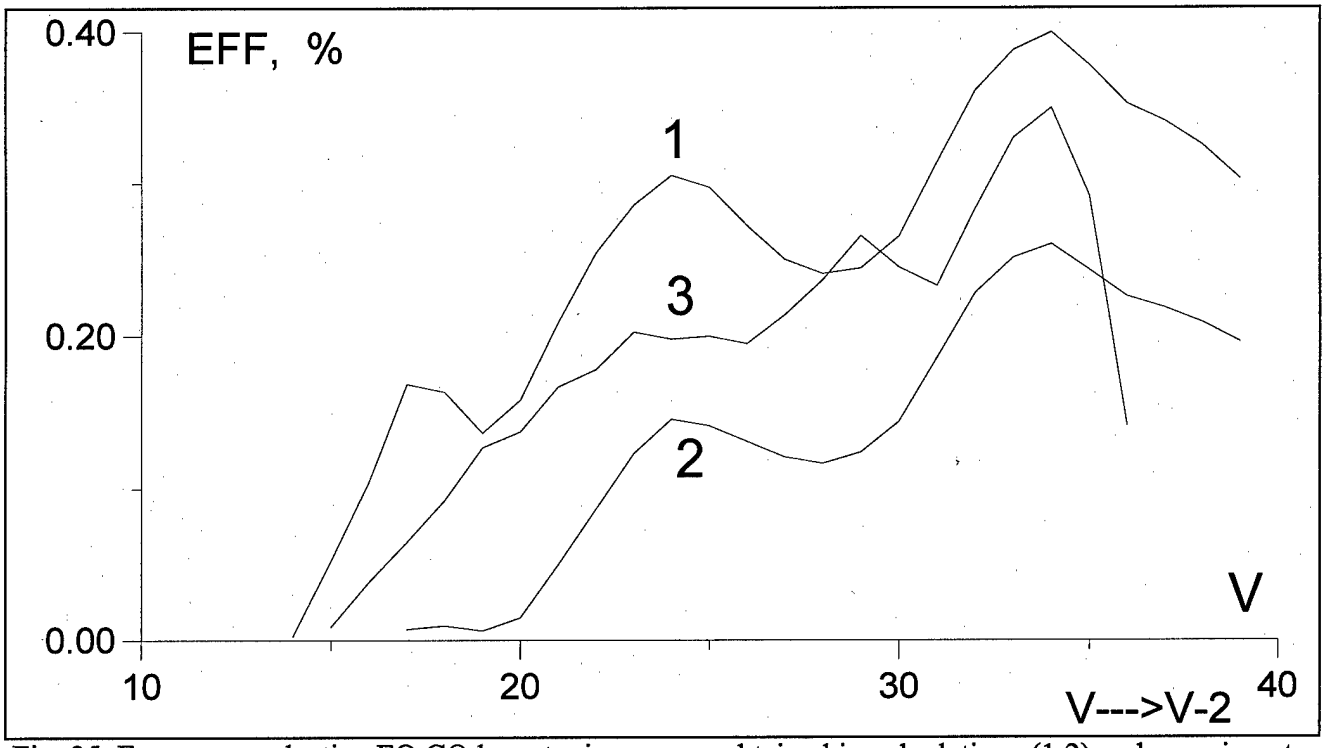

Fig. 25. Frequency selective FO CO laser tuning curves obtained in calculations (1,2) and experiment (3). $G_{th}=10^{-3}cm^{-1}$ (1) and $1.4\cdot10^{-3}cm^{-1}$ (2), MQE model.

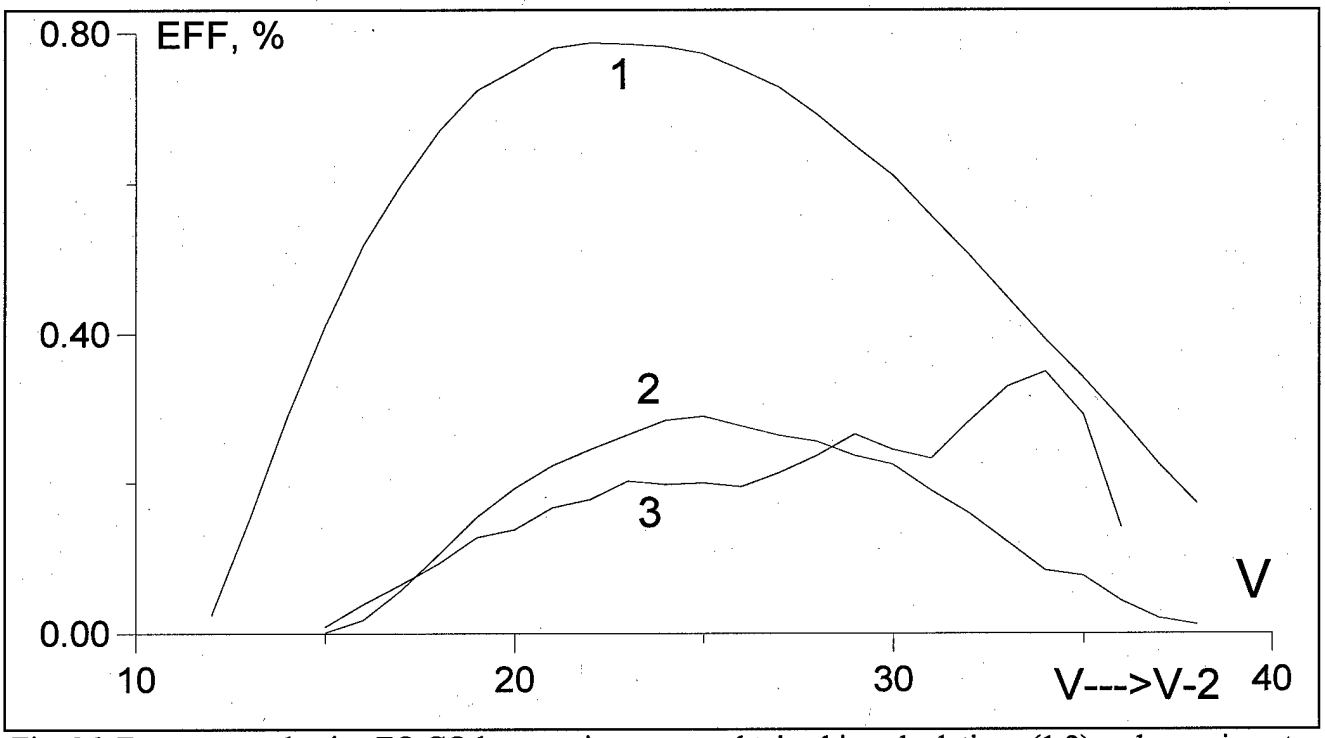

Fig. 26. Frequency selective FO CO laser tuning curves obtained in calculations (1,2) and experiment (3). $G_{th}=10^{-3}cm^{-1}$ (1) and $1.4\cdot10^{-3}cm^{-1}$ (2), SQE model

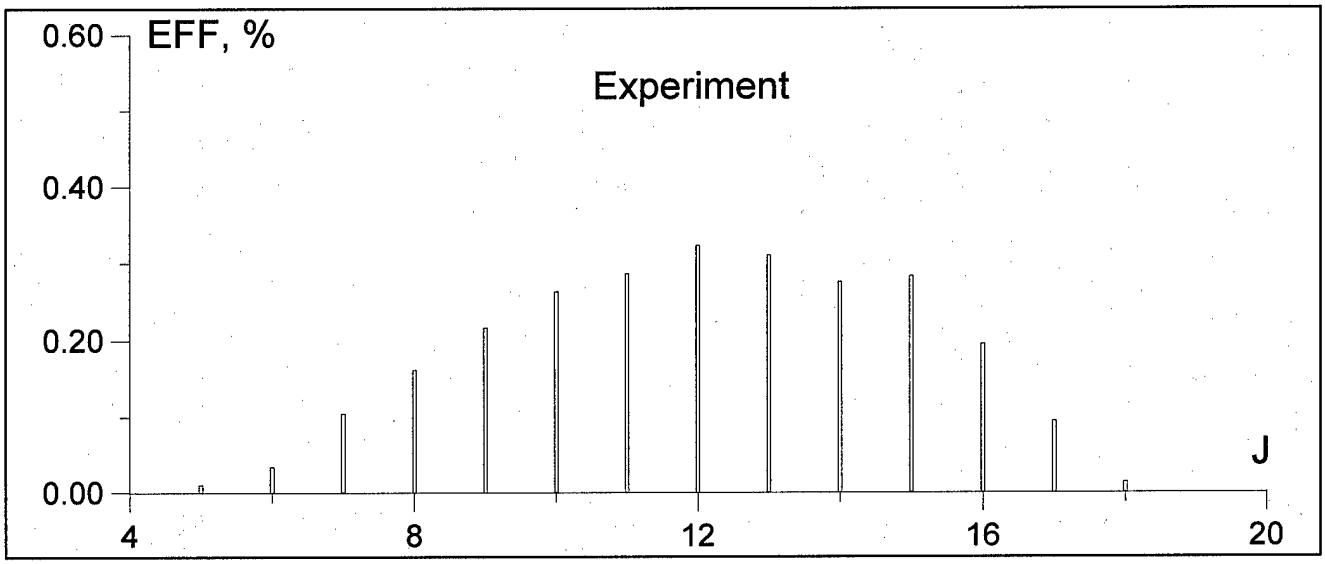

Fig. 27. Measured energy efficiencies for P-branch components in the band V→V-1=33→31.

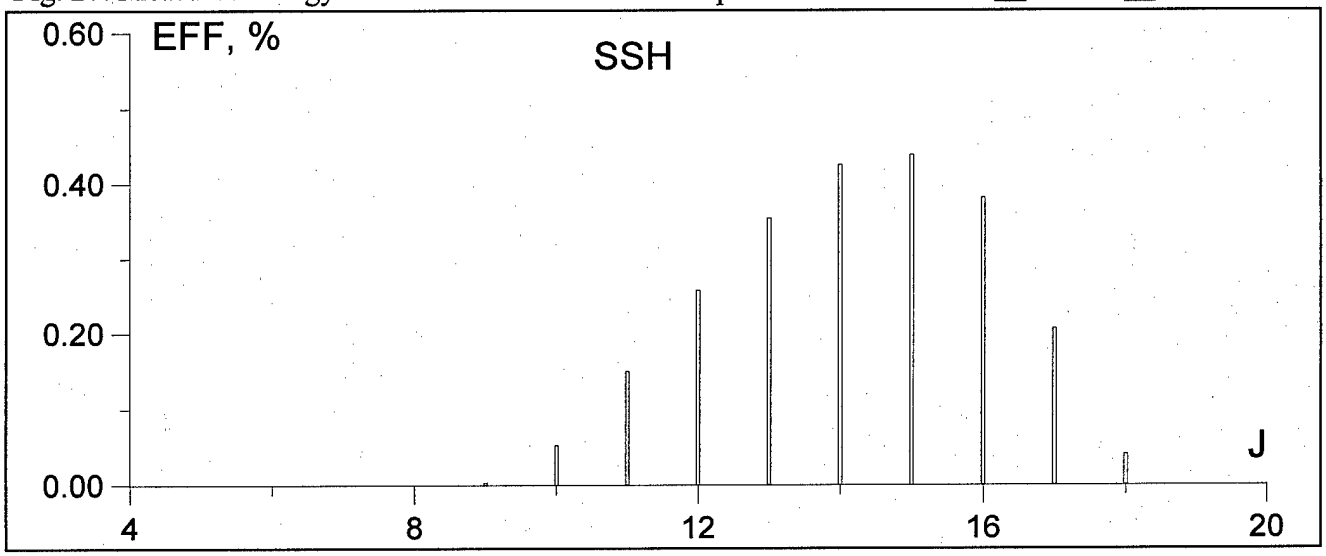

Fig.28. Calculated efficiencies for P-branch components in the band V→V-1=33→31, SQE model.

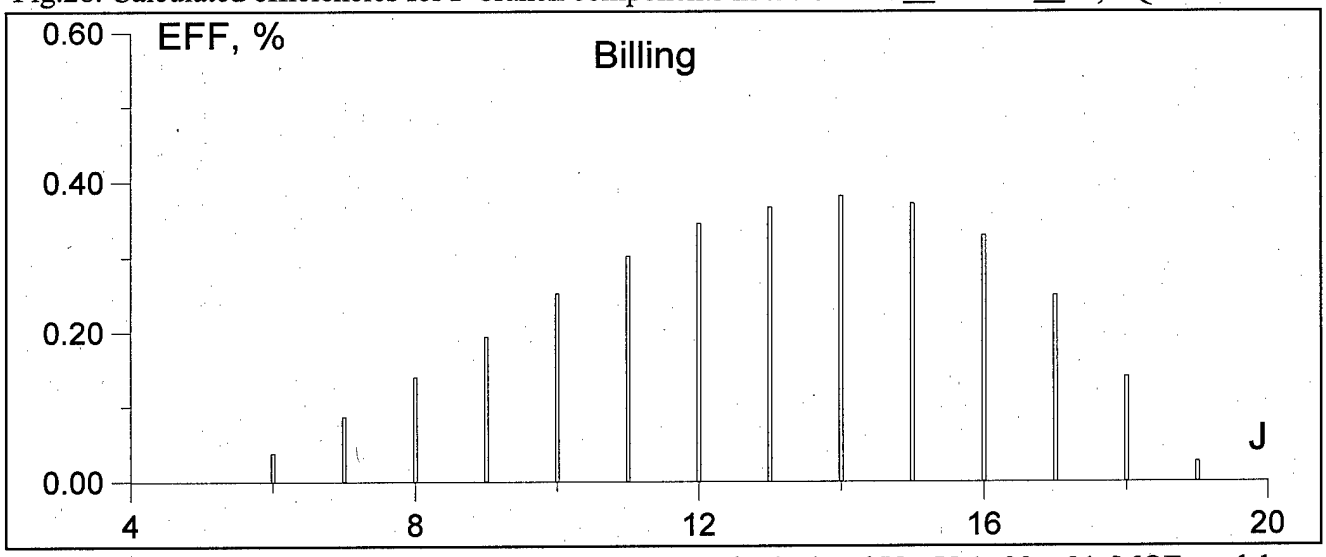

Fig.29. Calculated efficiencies for P-branch components in the band V→V-1=33→31, MQE model.

It is clearly seen that MQE model produced much better agreement with the experimental data than the old SQE one. It is very important that the computed curves manifest the same trend as in the experiments - they produce higher pulse energy for the higher transitions around **v**=34 while the old theory predicted a maximum around **v**=24. Bearing in mind uncertainties associated with a not sufficient knowledge of effective transmittance (reflectance) of the grating as a function of wavelength, the agreement between the predictions and measurements is rather good.

It is interesting to note that the MQE model improves also an accuracy of description of FO CO laser fine tuning within vibrational band $33 \rightarrow 31$. In Figs. 27-29 experimental data and results of calculations with the SQE and the MQE models are presented, respectively. Comparing theoretical predictions with the experiment, the conclusion can be made that the MQE model describes the measured data much more adequately.

6. CONCLUSIONS

Theoretical and experimental study on vibrational exchange kinetics of highly excited CO molecules has been performed by using double pulse Q-switching CO laser.

1. A comparison of experimental data on energy recovering ratio $R=Q_2/Q_1$ (Q_1 is an energy of the first-, and Q_2 is an energy of the second pulse of double pulse Q-switched CO laser producing a pair of short μs pulses with a variable time delay between them) with theoretical calculations obtained by using SQE model demonstrated for the first time, that this model is not valid for a description of Q-switched CO laser beginning with the vibrational level number **v**=14 and higher.

2. A set of kinetic rate constants needed for a theoretical description of CO laser was obtained by extrapolating and interpolating Billing's constants. These constants, also called by us as Billing's ones, were incorporated for the first time into kinetic equations within a framework of MQE model of CO laser taking into consideration multi-quantum exchange with the number of exchanged vibrational quanta m=1, 2, 3, 4. The MQE model was shown to result in quite different values of $R=Q_2/Q_1$ ratio as compared to SQE model.

3. A comparison of theoretical calculations, based on the MQE model with experimental data on R ratio obtained for a few selected vibrational-rotational transitions of CO molecule from **v**=8 up to **v**=20, demonstrated an adequate coincidence between them, giving the first direct evidence in support of the MQE model with Billing's constants.

4. The developed MQE model was used for the first time for a description of tunable single line first-overtone (FO) CO laser, demonstrating much better coincidence with experimental data for laser efficiency as function of vibrational and rotational numbers.

5. In the course of the research work some limitations of the experimental methodology were found. The ways to overcome these limitations are discussed below.

The first limitation is associated with a comparatively high cavity threshold gain caused by higher optical losses in the spectrally selecting unit of the laser resonator. A large amount of experimental data was obtained, when small signal gain but slightly exceeded the threshold gain. In such conditions one could not expect to get reliable results. The reproducibility of the experimental data was not very good (particularly, at the shortest delay time $\tau_{1\text{-}2}<2$ μs) and statistical error might reach up to ~50% in some cases. Therefore, a usage of the results of the experimental measurements to improve or correct magnitudes of the rate coefficients is questionable at present. The reason is not

quite full specification of laser cavity parameters and a limited accuracy of data. Diminishing these drawbacks may allow us to exploit laser experiments for refinement of modelling.

Secondly, in many cases single line selective Q-switching process did not possess a sufficiently high frequency resolution, thus preventing from the measurements of R ratio for a single selected line. Perturbation of the VDF by the first pulse frequently may cause an increase of the gain of adjacent spectral transitions, coupled by radiative cascade between vibrational levels and stimulate lasing for them. Besides, many spectral lines of CO molecules overlap occasionally. A modernization of the optical scheme (installing telescope in spectrally selecting unit) allowed us partially to improve the situation and obtain experimental data for a larger number of vibrational transitions. However, it was done at expense of intracavity loss increase.

It means that the method of double Q-switching of CO laser resonator still has a potential to be improved and serve as a good source of new kinetic information, in particular, for v-numbers up to v=33-37. The problem is how to decrease resonator losses. This may be done, for example, by substitution of aluminum rotating mirror by Au-coated one. One should remember also about a necessity to provide high spectral selectivity of the resonator. Therefore, the most actual problem is the problem of increasing Q-factor of the resonator containing a beam expander serving for high spectral selectivity.

An analysis performed for both types of the experiments (double-pulse procedure and FO laser tuning curve) clearly demonstrated that the results of numerical simulations are quite sensitive to the particular choice of the model for VV exchange (SQE/MQE). A striking result of the research is, that multi-quantum VV exchange rate constants, calculated by Billing and extrapolated and interpolated by us, being incorporated in kinetic equations of CO laser, describe rather well a set of experimental data, both for double pulse Q-switching CO laser and single line tunable FO CO laser within the limits of uncertainty of the measurements. This result was not evident in advance, because the extended Billing's rate constants were calculated using a lot of approximations, the validity of which should be verified by measurements.

A set of VV exchange rate constants existing at the moment was obtained by not strictly approved procedure of interpolation and extrapolation of the data calculated and published in [6]. Some processes were ignored because of scarce information about them. Generally, a full set of processes should be included in the model to treat quite reliably experimental data. Further more

precise determination of VV exchange rate constants is important not only as a basic problem, but also as an applied problem to improve FO CO laser modeling, especially single line selective FO CO laser. In the last case, the exact knowledge of kinetic processes for CO molecules excited as high as the 40-th vibrational level is necessary.

The more versatile way to improve the situation is the use of master oscillator - laser amplifier (MOLA) technique for measuring experimentally the VDF relaxation process perturbed by strong radiation on selected vibrational-rotational transitions. By doing this, we can get rid of the high-threshold effects and achieve higher accuracy of the measurements. In the MOLA methodology it is supposed gain recovery in laser amplifier cell to be measured after perturbation by a strong saturating laser pulse. Keeping in mind that data on high excited levels kinetics is particularly interesting, gain recovery dynamics should be measured using fundamental bands and FO transitions in a wide v-number range. This objective is a challenge to our capabilities at the moment and its solution would require a special research program. In the course of work under research program, new experimental tools and diagnostic methods should be developed. It is expected that quite extended set of experimental data would be obtained experimentally and evaluated theoretically.

7. REFERENCES

1. W.Q.Jeffers, J.D.Kelley. J.Chem.Phys., v.55, p. 4433 (1971)
2. W.B.Lacina, M.M.Mann, G.H.McAllister. IEEE J., v.QE-9, p. 588 (1973)
3. Yu.B.Konev, I.V.Kochetov, V.G.Pevgov, V.F.Sharkov. I.V.Kurchatov Atomic Energy Institute. Preprint 2821, Moscow (in Russian) (1977)
4. N.S.Smith, H.A.Hassan. AIAA Journ., v. 14, p. 374 (1976)
5. T.A.Dillon, J.C.Stephenson. Phys.Rev.A, v.6, p.1460 (1972)
6. G.D.Billing.. In: Non-equilibrium vibration kinetics. Ed. by M.Capitelli. Springer, Berlin, 1986, Ch.4.
7. Yu.B.Konev, I.V.Kochetov, A.K.Kurnosov, B.A.Mirzakarimov. J. Phys. D:Appl. Phys., v. 27, pp. 2054-2059 (1994).
8. Yu.B.Konev, I.V.Kochetov, A.K.Kurnosov, B.A.Mirzakarimov. Quant. Electr. v. 24, pp. 124-127 (1994)
9. A.A.Ionin, Yu.M.Klimachev, Yu.B.Konev, A.K.Kurnosov, I.V.Kochetov, V.D.Sinitsyn. Double pulse lasing in single line Q-switched CO laser. Proceedings of the International Conference on LASERS'97. Ed. J. J. Carroll & T. A. Goldman. STS Press/McLean, VA, 1998, pp. 88-91.
10. A.A.Ionin, Yu.M.Klimachev, V.D.Sinitsyn, A.K.Kurnosov, I.V.Kochetov, Yu.B.Konev. XI International Symposium on Gas Flow and Chemical Lasers and High Power Laser Conference, Edinburg, UK, 1996, Proc. SPIE 3092, p. 301 (1996).
11. A.Ionin, Yu.Klimachev et al. Experimental and theoretical study on first overtone carbon monoxide laser physics. Lebedev Physical Institute. Preprint N11, Moscow, 1998.
12. R.Farrenq, C.Rossetti, G.Guelashvili, W.Urban. Chem. Phys., 1985, v. 92, p. 389.
13. G.V.Dubrovskiy, A.V.Bogdanov. A general quasi-classical approximation of the T-operator in angle-action variables. Chem. Phys. Lett., 1979, v. 62, pp. 89-94.
14. A.V.Bogdanov, Yu.E.Gorbachev, V.A.Pavlov. To the theory of vibration and rotation quanta exchange in the molecular collisions. A.F.Ioffe Institute of Physics&Technology. Preprint N833, Leningrad, 1983.
15. P.Crowell. Kinetic Rates for Rotational and Vibrational Relaxation of CO. Memo on Contract F29601-95-C-0197, CDRL A005.
16. Yu.B.Konev, I.V.Kochetov, V.S.Marchenko,V.G.Pevgov, V.F.Sharkov. The main characteristics of CO laser gas discharge plasma. I.V.Kurchatov Inst. Atom. Energy. Preprint IAE N 2810, Moscow, 1977 (in Russian).
17. K.F.Herzfeld, T.A.Litovitz. Absorption and Dispersion of Ultrasonic waves. N.Y., 1959.
18. N.G.Basov, V.G.Bakaev et al. J. of Tech. Phys., v. 55, p. 326, 1985 (in Russian).